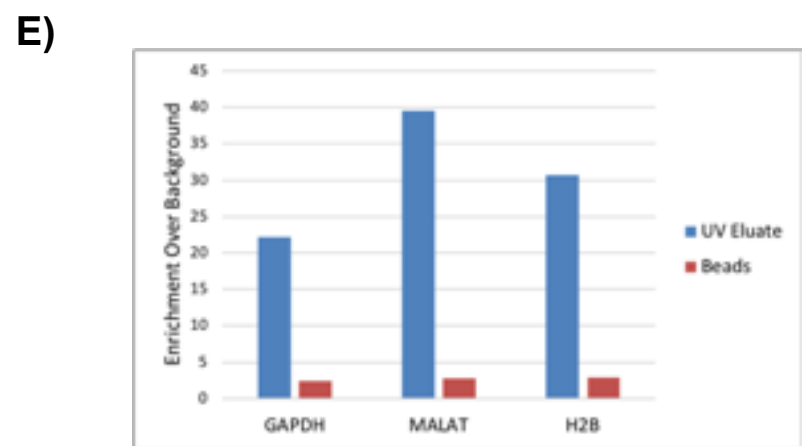
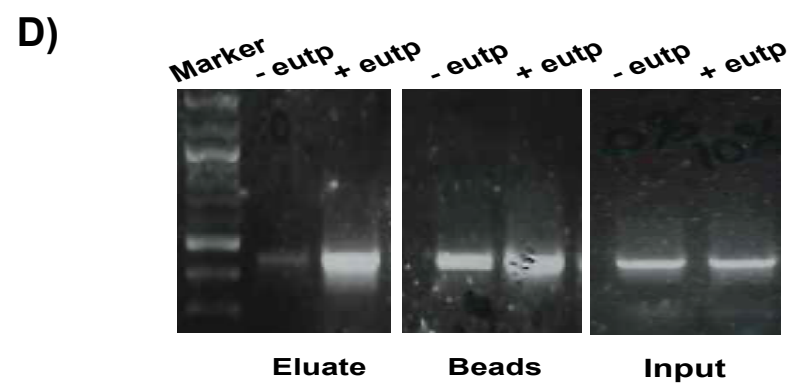
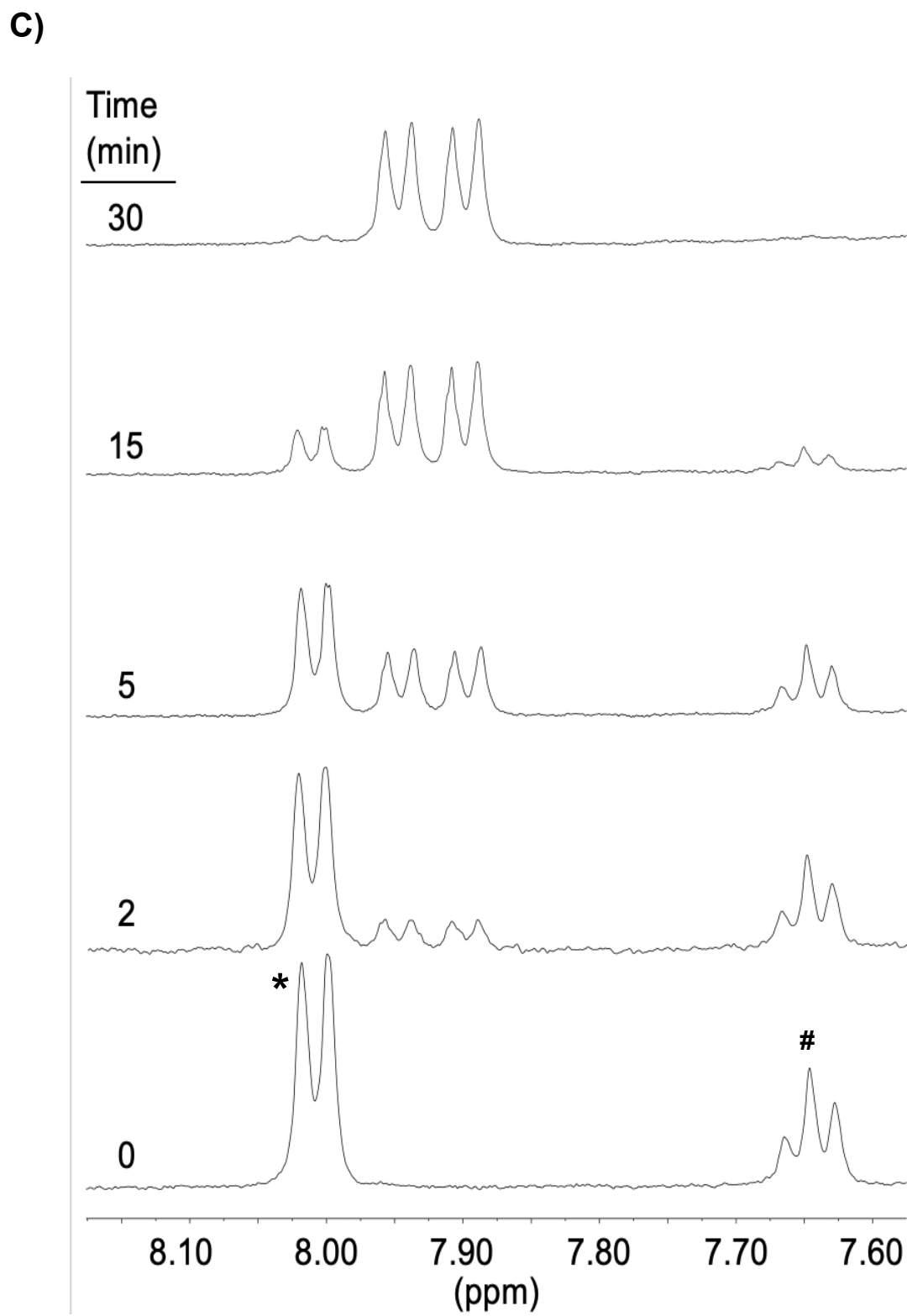
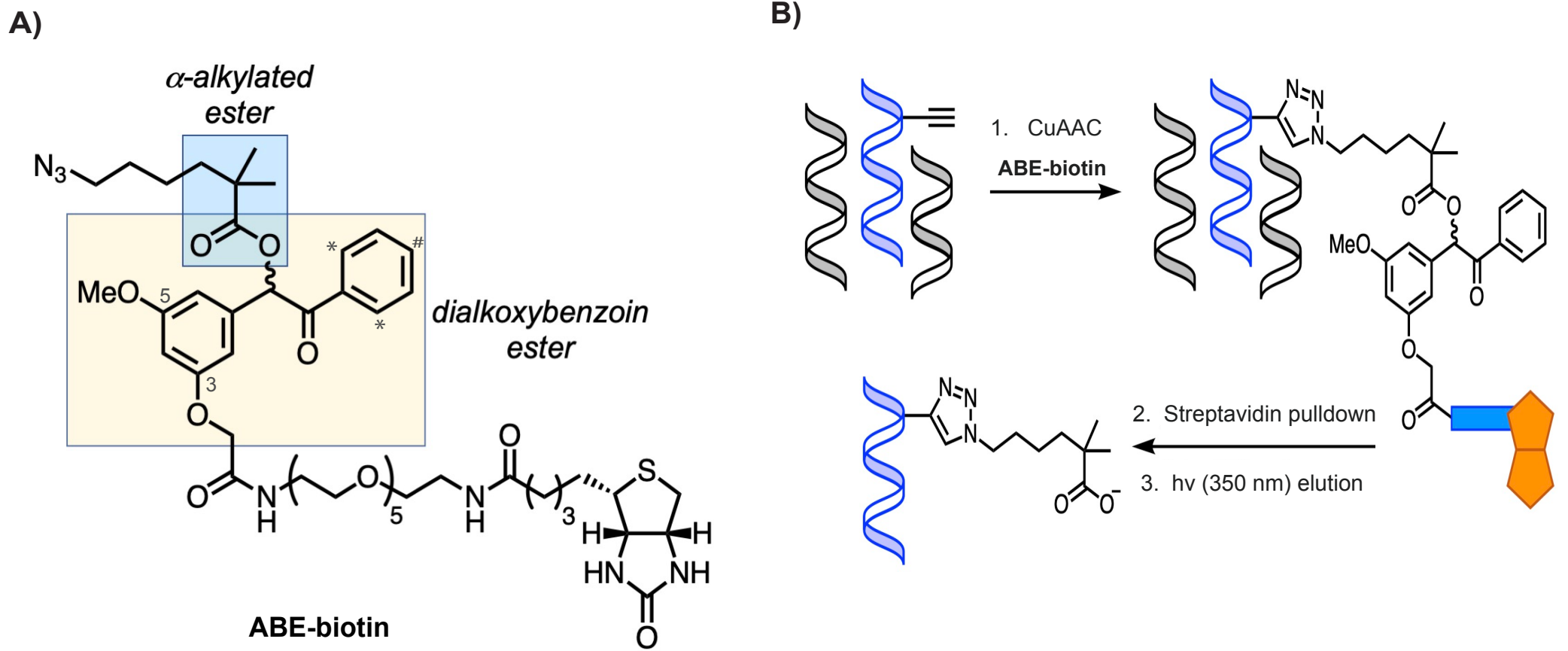


Supplemental Information

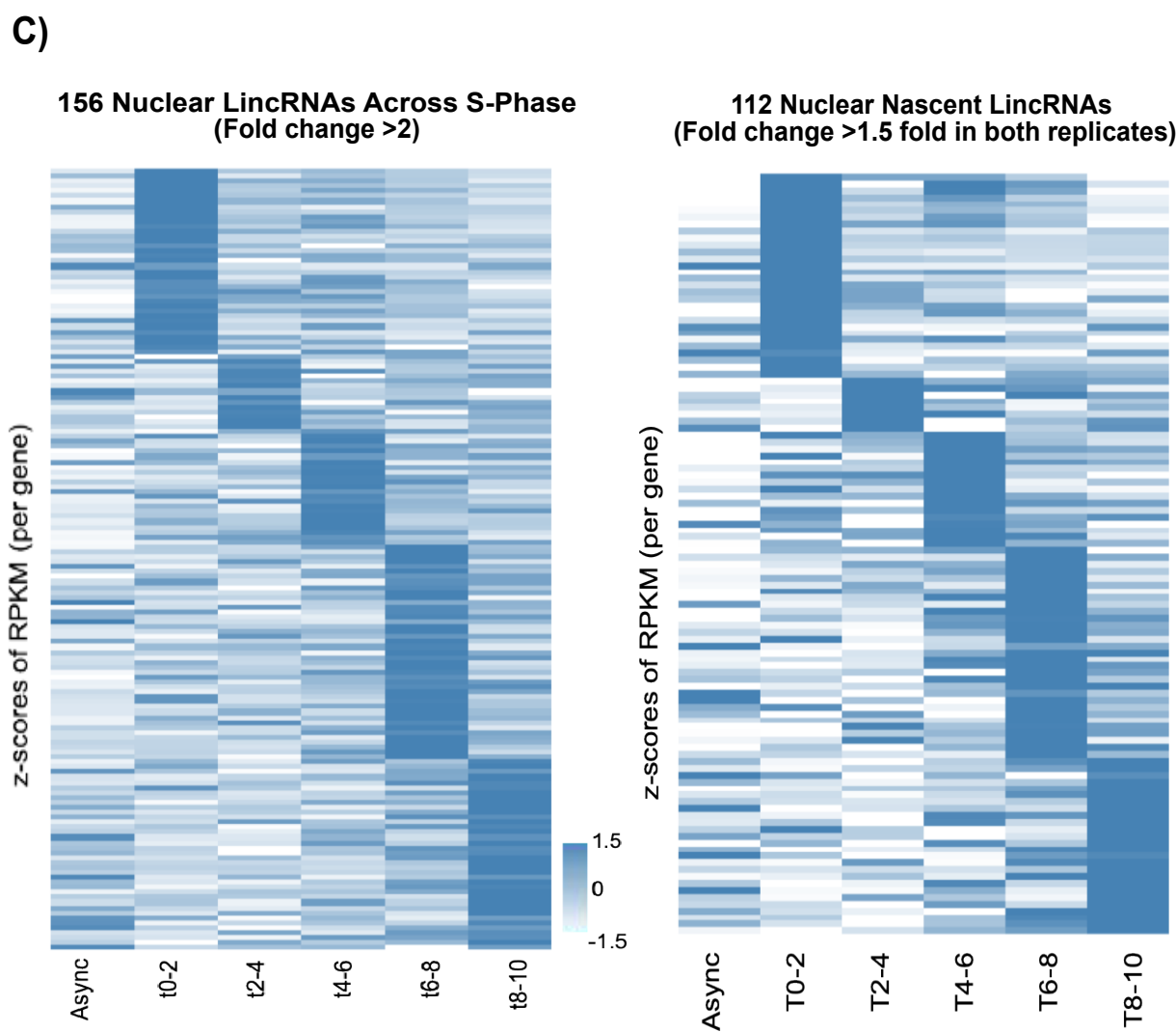
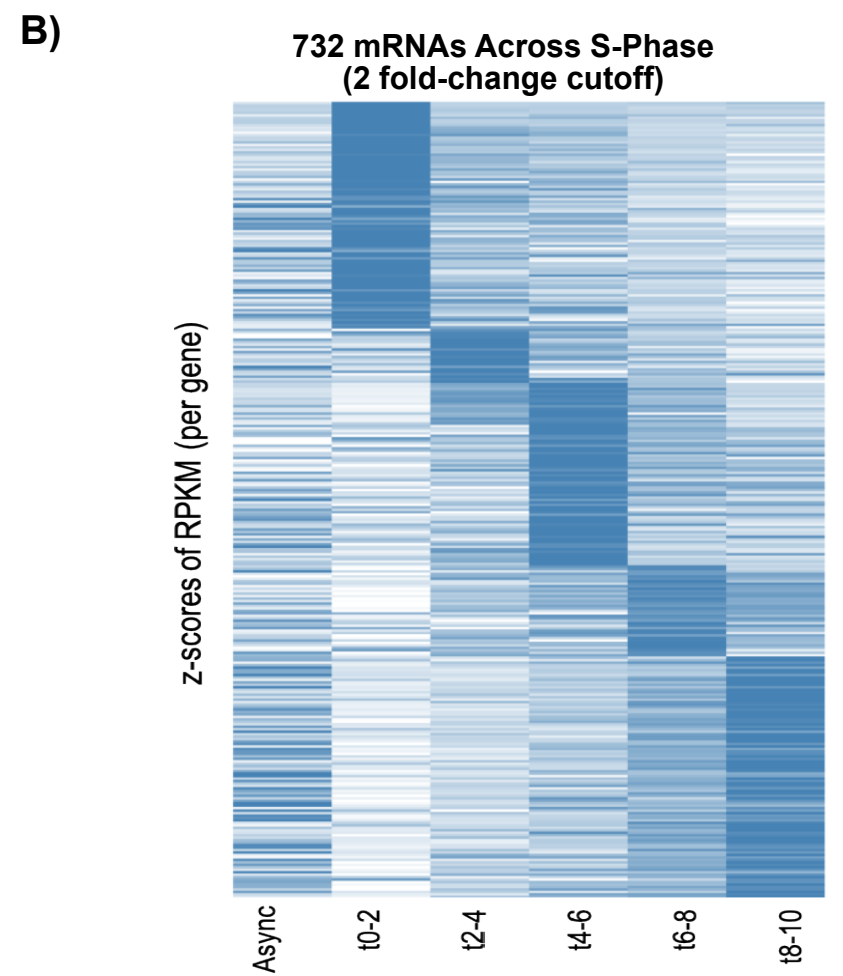
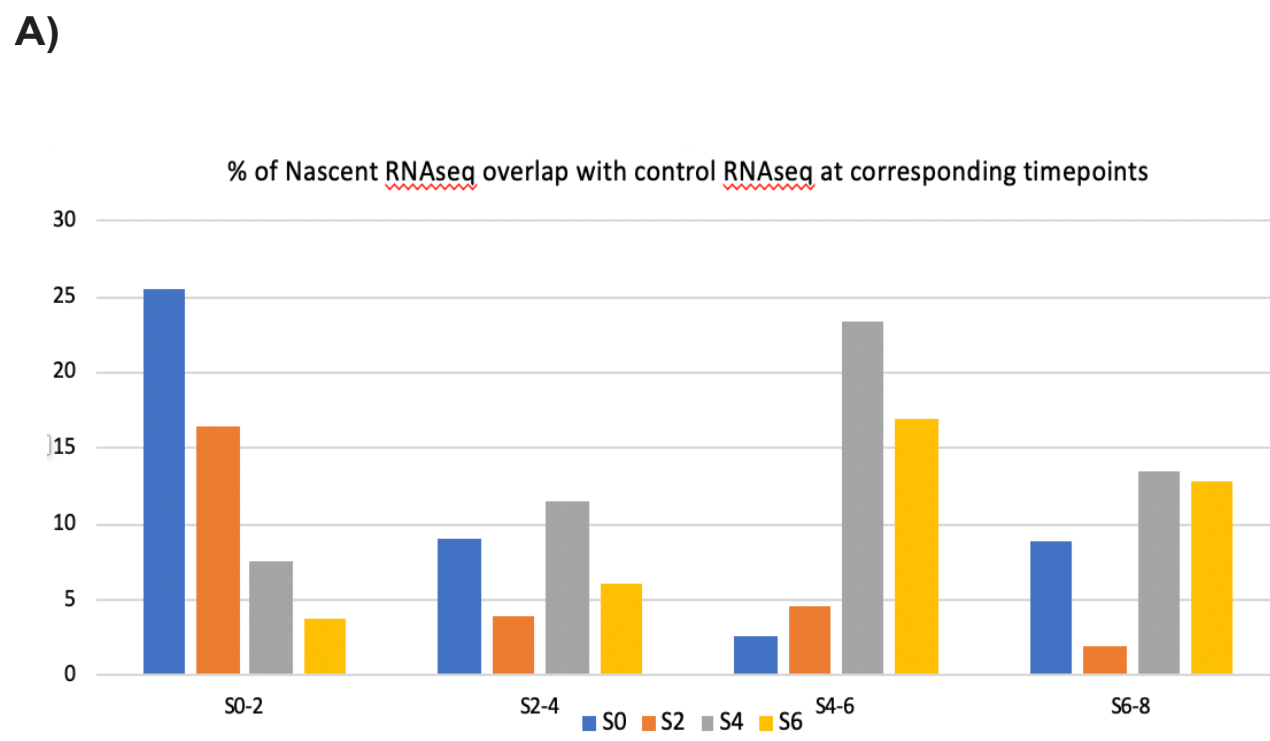
S-phase enriched non-coding RNAs regulate gene expression and cell cycle progression

Ozlem Yildirim, Enver C Izgu, Manashree Damle, Vladislava Chalei, Fei Ji, Ruslan I. Sadreyev, Jack W. Szostak, Robert E. Kingston



Supplementary Figure 1, Related to Figure 1

A) Structure of the azido-biotin probe, ABE-biotin. For rapid photocleavage, we designed ABE-biotin with an α -alkylated ester group and a 3,5-dialkoxyphenyl core, as these chemical modifications were shown to accelerate the rate of UV-induced decarboxylation of benzoin esters (Shi, Corrie, & Wan, 1997) **B)** Schematic of the general protocol for labeling and isolation of the EU-labeled RNA using ABE-biotin. **C)** ^1H NMR (400 MHz, d_3 -acetonitrile/ D_2O 1:1 mixture) spectral overlay of the photolysis reaction of ABE-biotin using a bench-top Rayonet UV reactor. The doublet resonance at 8.14 ppm is from two, magnetically equivalent, *ortho*-Hs (*) of the phenone moiety and the triplet at 7.65 ppm is from *para*-H (#). Over the course of UV irradiation (350 nm), their peak intensities decrease while two separate doublet resonances at 7.95 and 7.90 ppm emerge, indicating the conversion of ABE-biotin into two potential benzofuran-derived (Shi et al., 1997) photolysis products. This is likely due to the asymmetric nature of the parent benzoin core where the alkoxy substituents are different (C3 vs C5). Over 95% of ABE-biotin was converted into these photolysis products within ca. 30 min of UV irradiation. **D)** EU labeled nascent RNA is enriched over background significantly by UV elution. RNA molecules *in vitro* transcribed with or without ethynyl uridine triphosphate (+ eutp and – eutp respectively). ABE-biotin probe covalently attached to eu incorporated RNA via click chemistry; then labeled molecules were pulled down with streptavidin magnetic beads. While the - eutp eluate does not show any amplification (first gel, band on the left), when reaction is proceeded on beads - eutp samples show significant nonspecific amplification (second gel band on the left). First gel, band on the right, + eutp eluate, shows the effectiveness of photolysis when ABE-biotin was used as the isolation tool. **E)** Comparison of eluates versus beads enrichment over background is compared with qPCR in pulldown samples followed after *in vivo* metabolic labeling.



D)

G1/S border (t0-2hr)

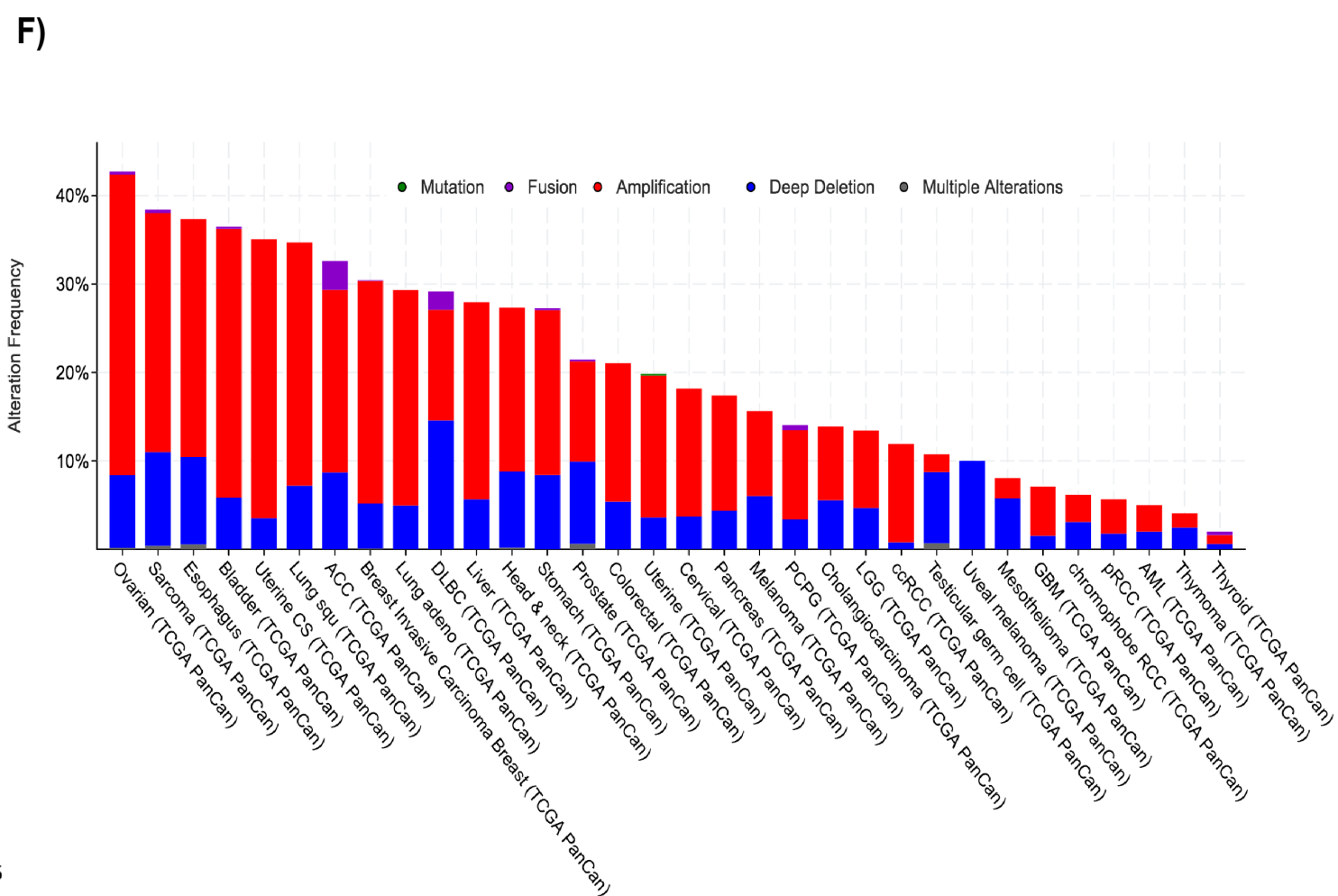
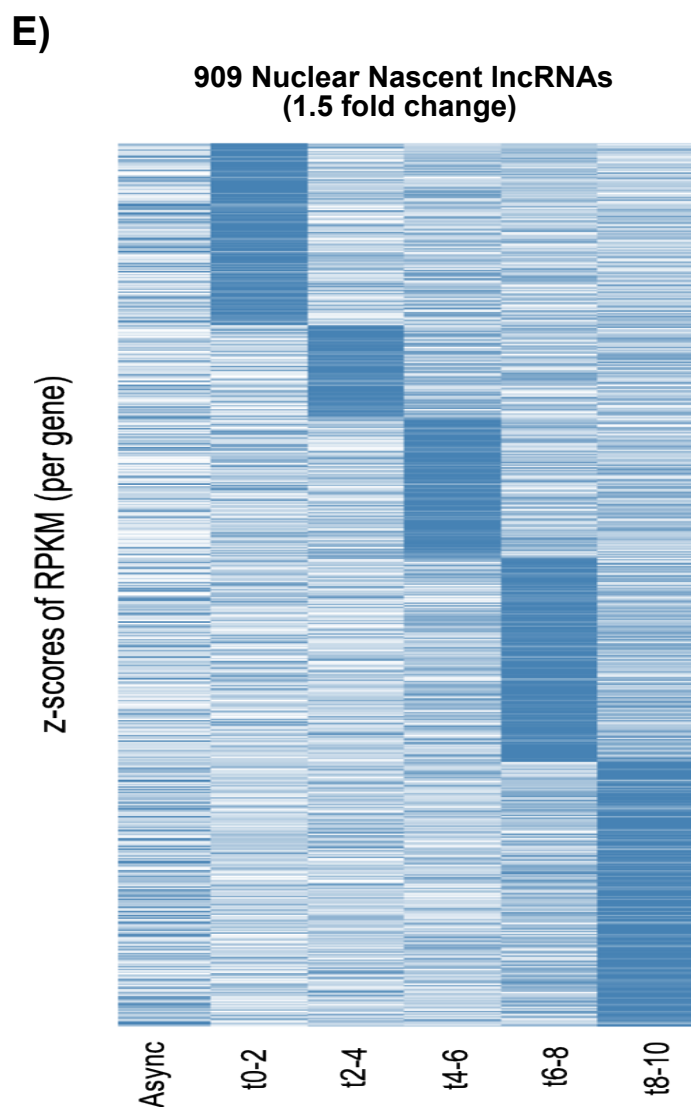
Biological Process	p-value
Multicellular Organism Development	1.60E-14
Negative Regulation of Cellular Metabolic Process	9.60E-15
Anatomical Structure Development	1.80E-14
Developmental Process	1.80E-14
Macromolecule Biosynthetic Process	2.30E-13

Early S (t2-4hr & t4-6hr)

Biological Process	p-value
Nucleosome Assembly	5.10E-16
Chromatin Assembly	8.70E-15
Nucleosome Organization	7.10E-15
DNA Packaging	6.40E-13
Protein-DNA Complex Assembly	1.60E-12

Mid/Late S (t6-8hr & t8-10hr)

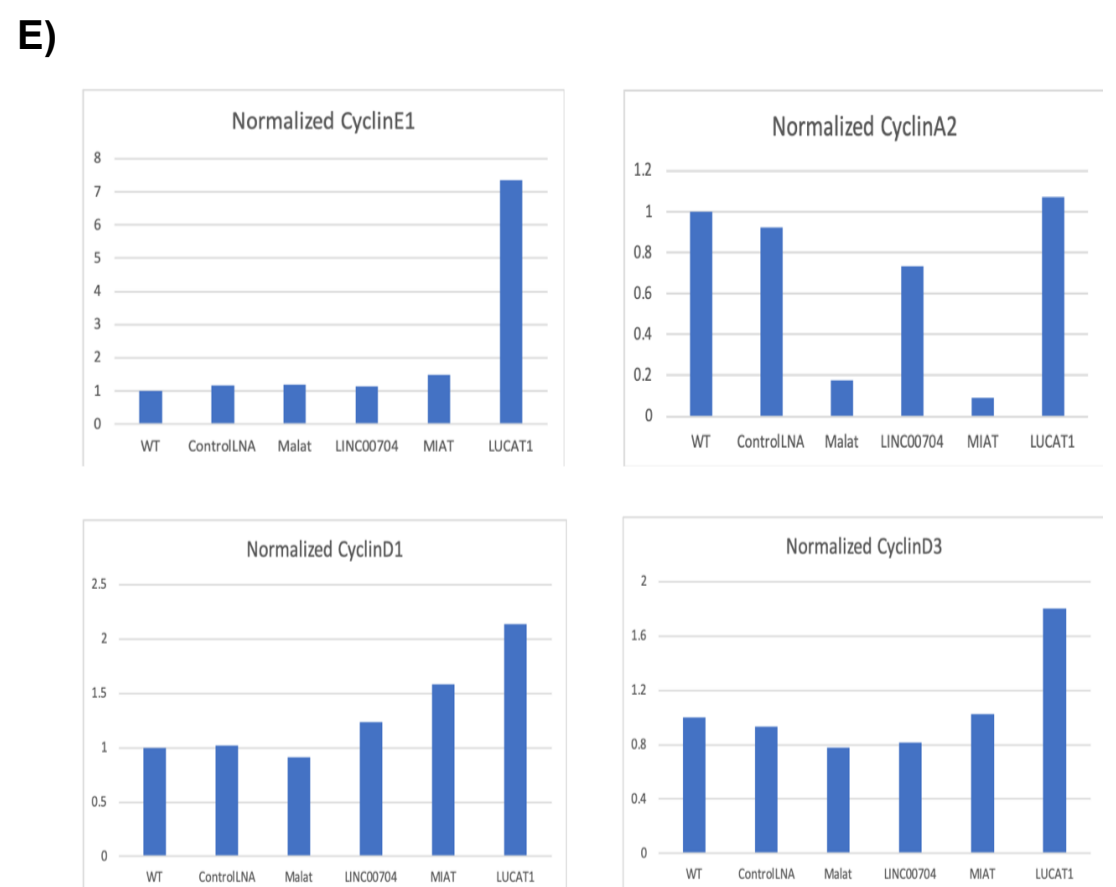
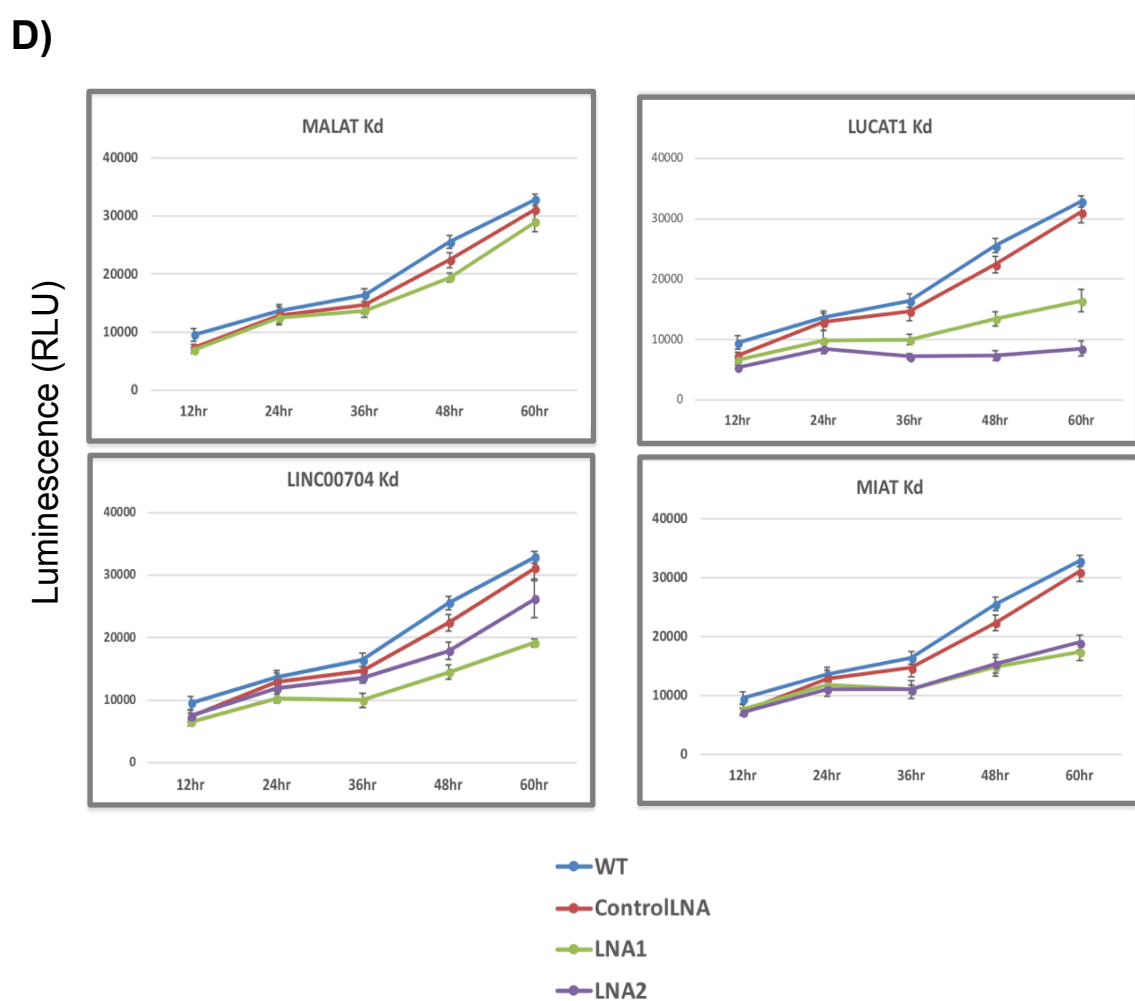
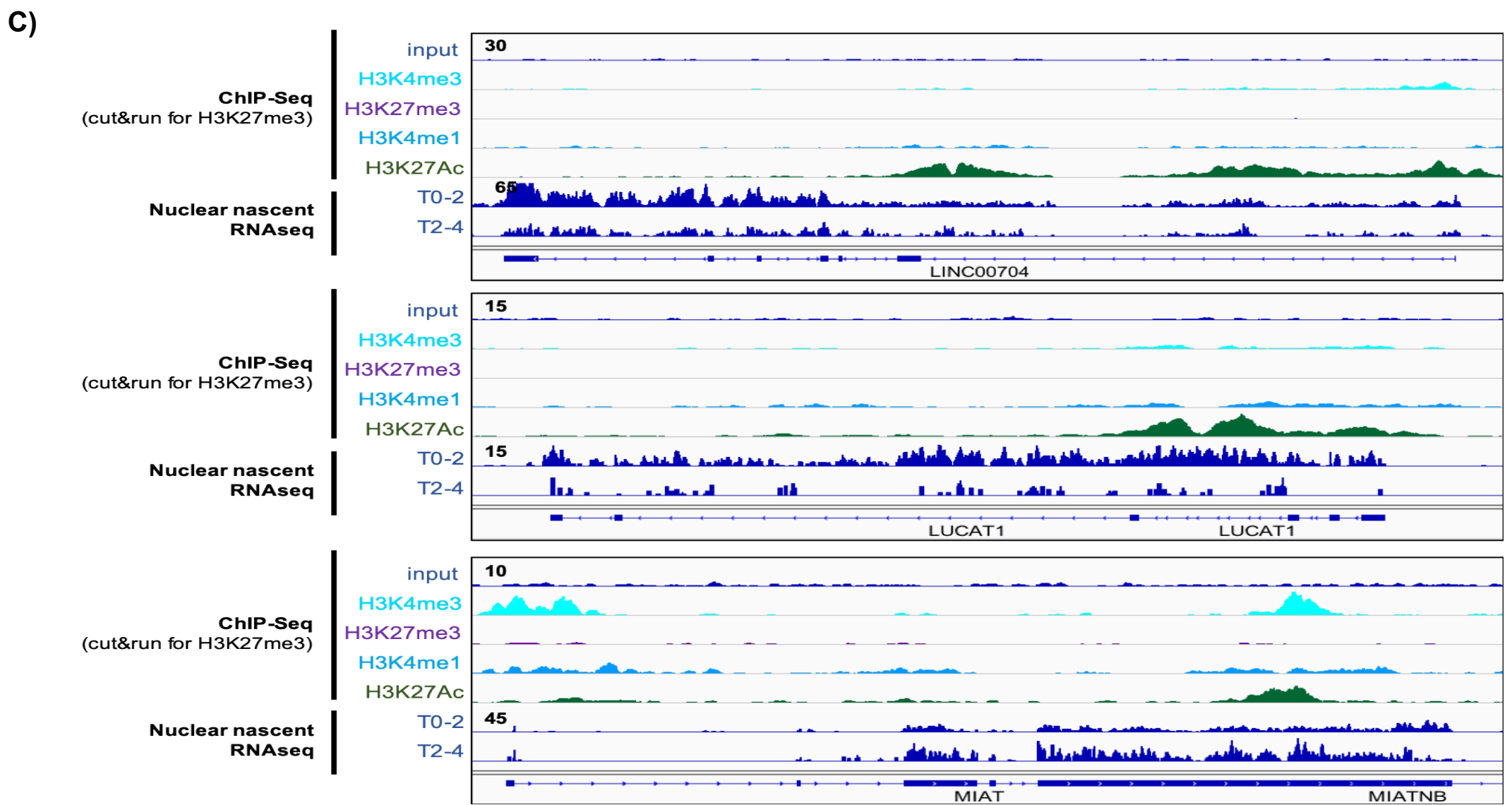
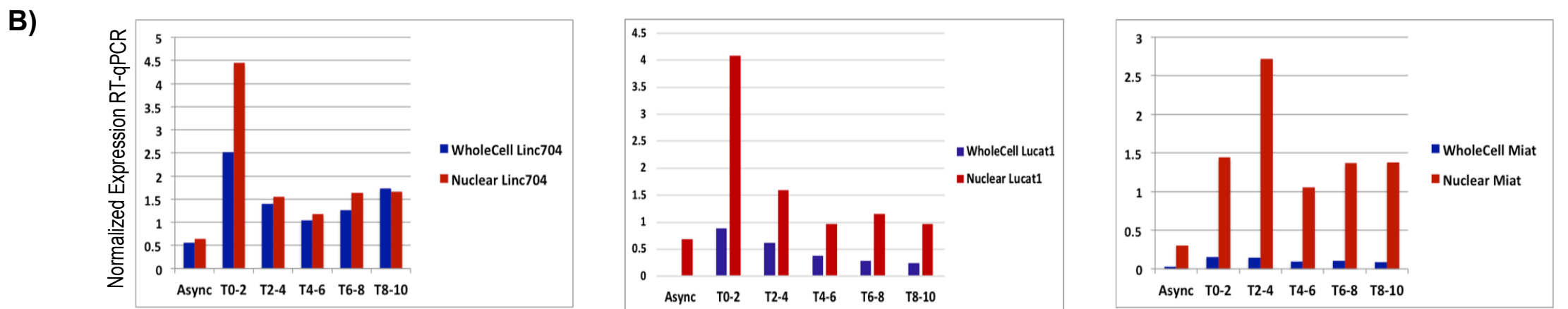
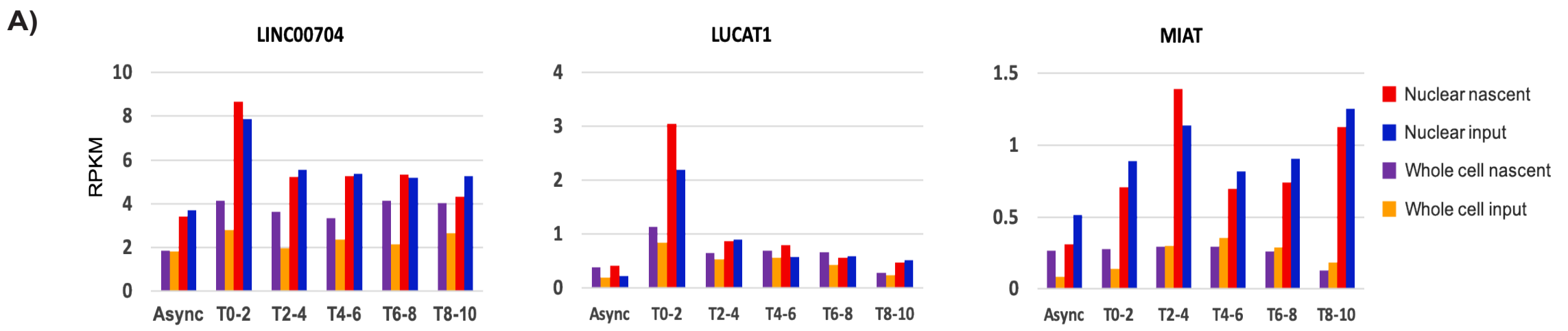
Biological Process	p-value
ncRNA Metabolic Process	9.40E-28
RNA Processing	9.90E-26
Organelle Organization	1.10E-23
Gene Expression	1.10E-23
Mitotic Cell Cycle Process	8.80E-20



Supplementary Figure 2, Related to Figure 2

A) Overlap of gene expression peaking at different time points of S-phase in WT cells and control LNA transfected cells. For each time point in WT cells, overlap with each time point in control cells is shown as percentage of total overlapping genes. Most genes in WT and Control cells peak at similar time points, showing that the results are reproducible. **B)** Whole cell nascent mRNA expression profiles for differentially expressed genes across S-phase time course (maximum RPKM/minimum RPKM > 2). Z-score of average of two replicates per time point is shown and genes are clustered based on the time point of the maximum expression level **C)** Nuclear nascent lincRNA expression profiles for differentially expressed genes across S-phase time course (maximum RPKM/minimum RPKM > 2 on the left, upregulated >1.5 fold in both replicates per time point on the right). Z-score of average of two replicates per time point is shown and ncRNAs are clustered based on the time point of the maximum expression level. **D)** Gene Ontology terms of nascent mRNAs clusters in each time point. **E)** Nuclear nascent lincRNA expression profiles for differentially expressed genes across S-phase time course (maximum RPKM/minimum RPKM > 1.5). Z-score of average of two replicates per time point is shown and genes are clustered based on the time point of the maximum expression level **F)** Alteration frequencies of S-phase enriched lincRNAs in TCGA database.

Yildirim et al. Supplementary Figure 3

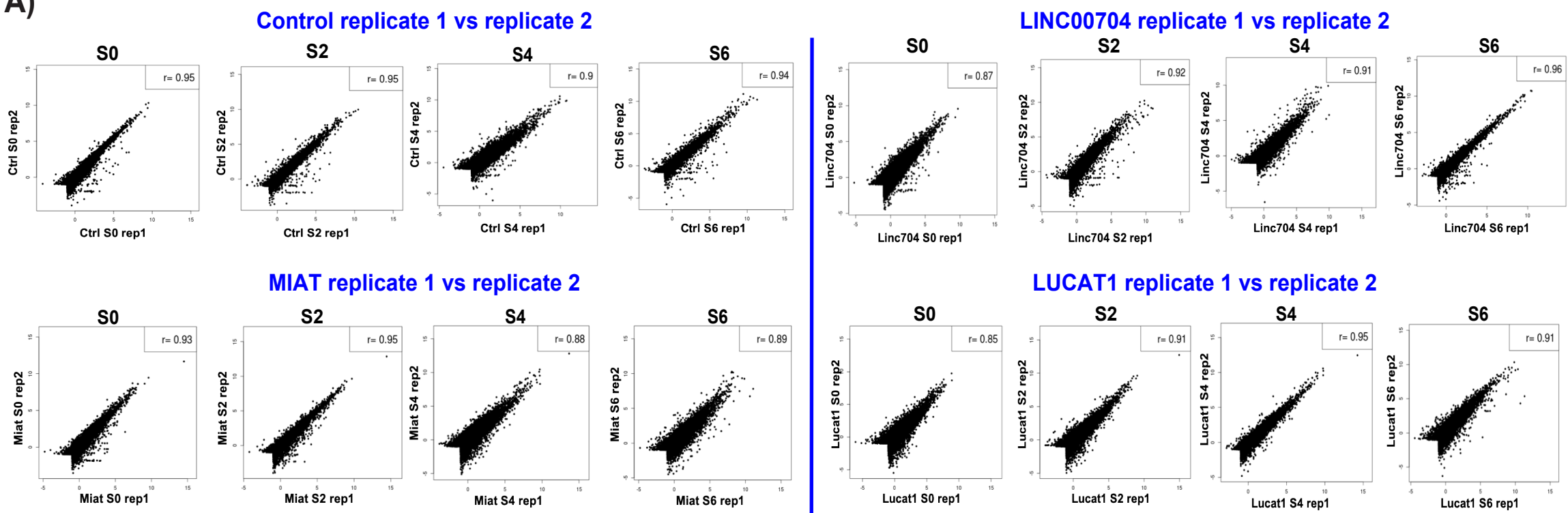


Supplementary Figure 3, Related to Figure 3

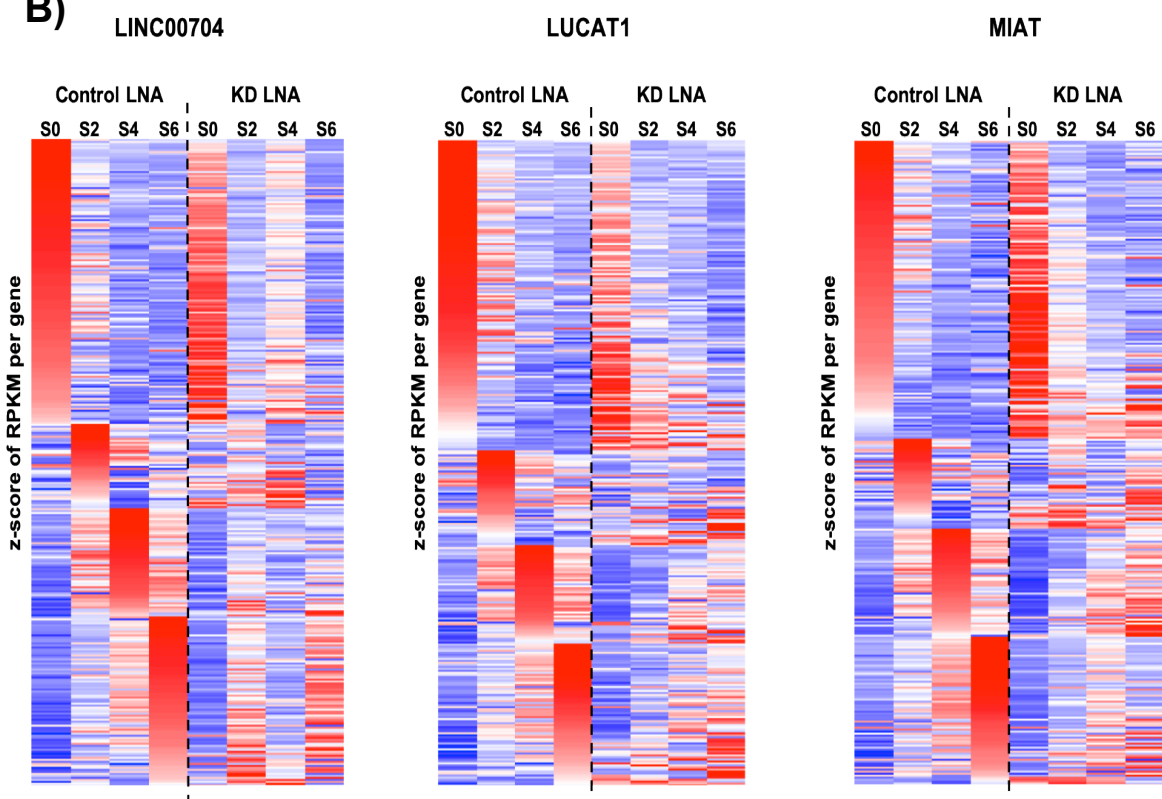
A) Whole cell and nuclear nascent pulldown and input RNA-seq bar plots across S-phase showing nuclear enrichment and the peak time of each Linc00704 LUCAT1 and MIAT and their levels are upregulated at early S-phase. **B)** Whole cell and nuclear rt-qPCR across S-phase shows Linc00704 and MIAT are nuclear enriched and their levels are upregulated at early S-phase. **C)** LINC00704, LUCAT1 and MIAT nascent RNA pull-down IGV tracks. **D)** Proliferation and cell viability assay showing different impacts of each lincRNA depletion on proliferation and viability. Asynchronous knockdown cells proliferation measured over the course of 60 hours. **E)** Quantification of western blots using ImageJ software.

Yildirim et al. Supp Figure 4

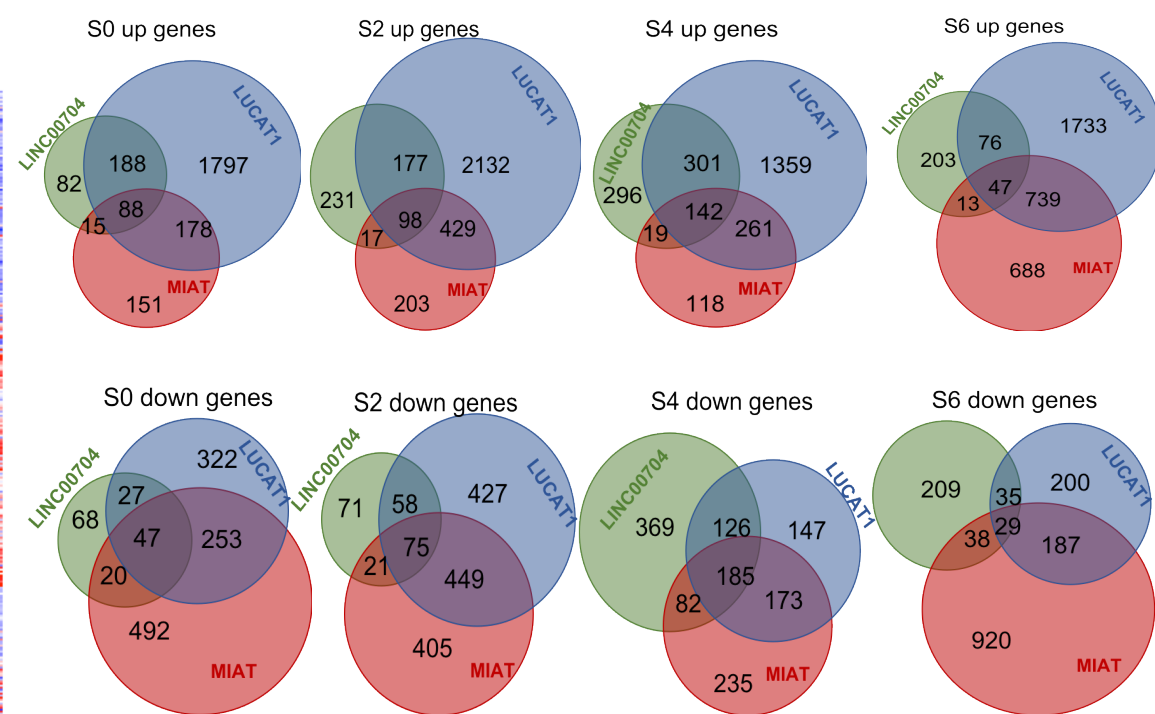
A)



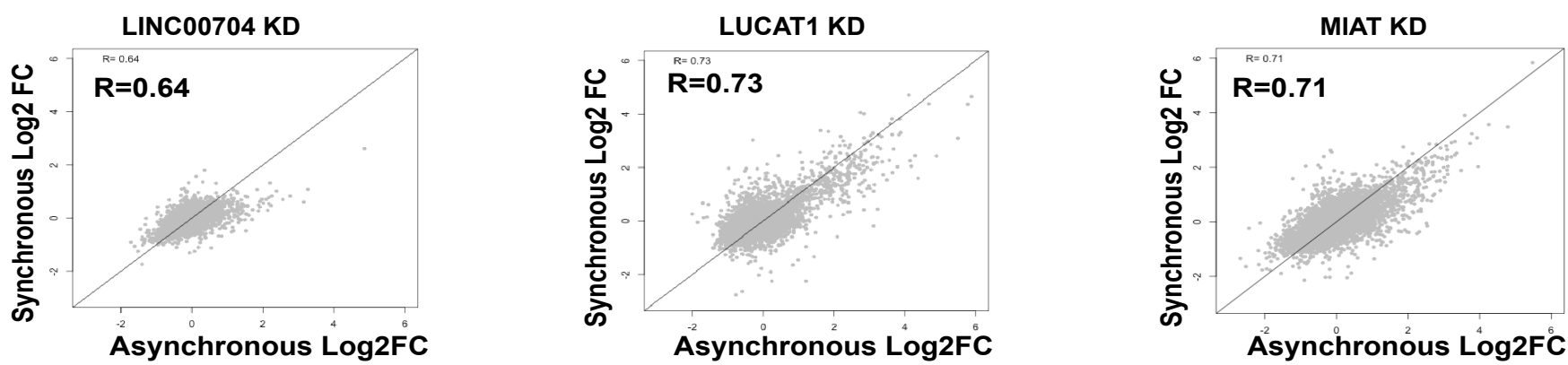
B)



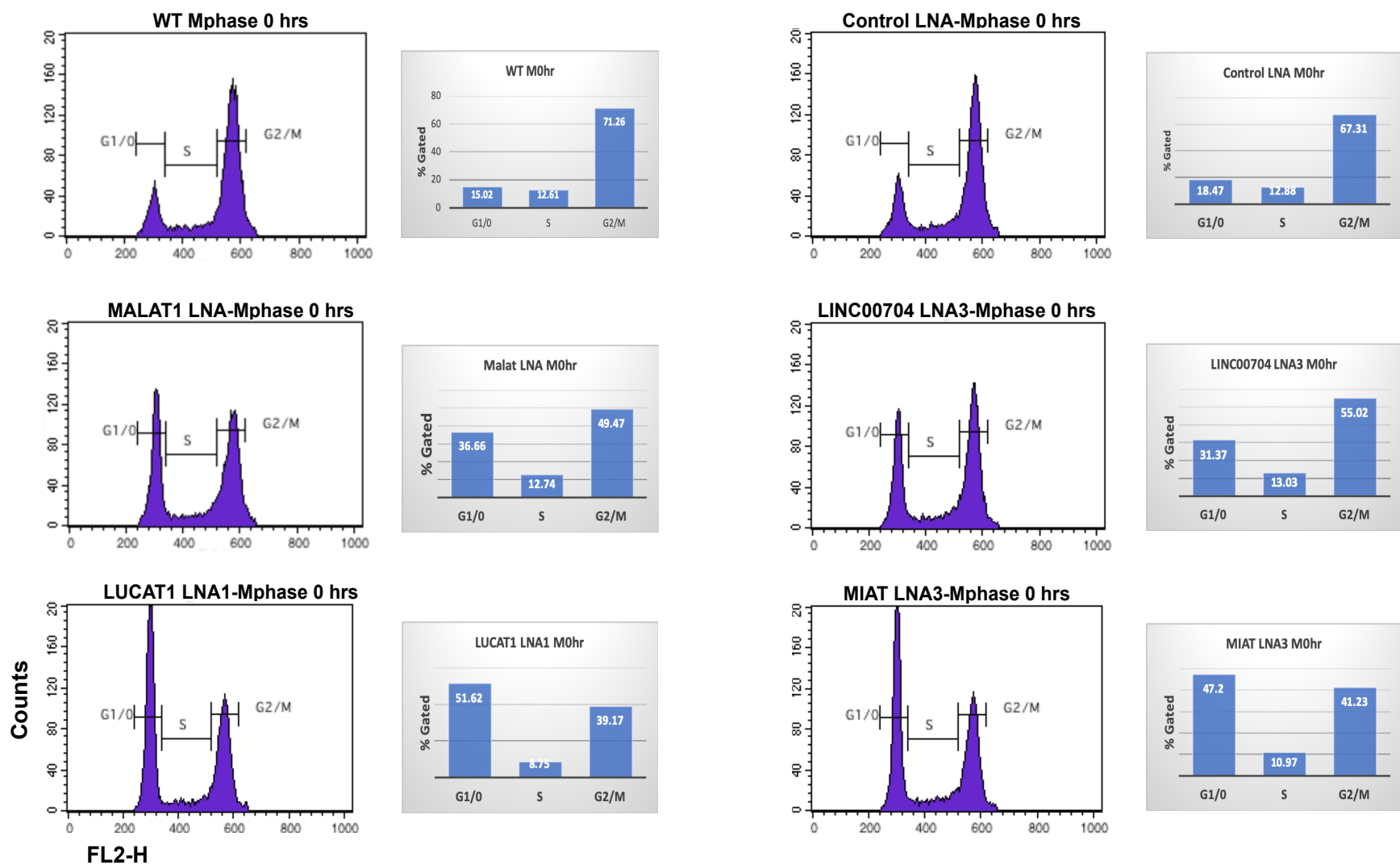
C)



D)



E)



Supplementary Figure 4, Related to Figure 4

A) Correlation plots of two biological replicates of strand specific RNA-seq experiments. **B)** Heat maps of strand specific RNA-seq clustered per their expression levels at 4 different time points in S-phase with more than 2-fold change in expression level in any time point in control cells.

C) Venn diagram showing overlap of differential genes upon Linc00704, LUCAT1 and MIAT knockdowns at different time points in S-phase. **D)** Correlation between regulation of genes in synchronous and asynchronous cells. log₂ fold-change knockdown over control is plotted for asynchronous cells and synchronous cells on the y-axis. For synchronous cells, average RPKMs of duplicates of all timepoints for control and triplicates for knockdown conditions were calculated. For asynchronous cells, average RPKM of duplicates was calculated for control and knockdown conditions. Pearson correlation coefficient is shown. **E)** 12hr after lincRNA or control LNA transfection, cells synchronized at M-phase with microtubule inhibitor TN-16 for 18hrs. Flow cytometry analysis showed efficient progression G1 and S-phase and synchronization at M-phase for wild type cells and control LNA transfected cells, while cells depleted of lincRNAs MALAT, LIN00704, LUCAT1 and MIAT fail to progress in S phase and synchronized at M phase.

Method S1. ABE-Biotin Synthesis (Related to Figure 1A and Supp Figure 1)

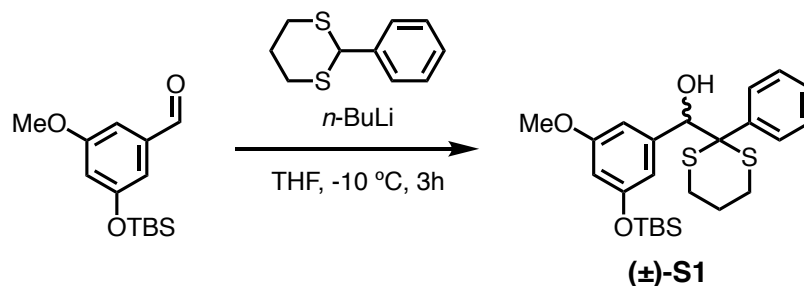
General Synthetic Methods

All reactions were performed under a dry argon atmosphere unless otherwise noted. All glassware was flame- and/or oven-dried before use. Pyridine (pyr), dimethylformamide (DMF), tetrahydrofuran (THF), dichloromethane (CH_2Cl_2), acetonitrile (CH_3CN), and triethylamine were purchased as anhydrous grade from Sigma-Aldrich. Methyl bromoacetate, 4-(dimethylamino)pyridine (DMAP), oxalyl chloride ($(\text{COCl})_2$), mercury(II) perchlorate hydrate ($\text{Hg}(\text{ClO}_4)_2 \cdot n\text{H}_2\text{O}$), 2-phenyl-1,3-dithiane, *n*-butyllithium (*n*-BuLi) in hexanes, tetrabutylammonium fluoride (TBAF), and potassium carbonate (K_2CO_3) were purchased from Sigma-Aldrich and used as received. Reagent grade ethyl acetate (EtOAc), hexanes, methanol (MeOH), CH_2Cl_2 , and diethyl ether were purchased from Fisher Scientific. Deuterated solvents were purchased from Cambridge Isotope Laboratories. 3-((*Tert*-butyldimethylsilyloxy)-5-methoxybenzaldehyde (Hurst et al., 2010), 6-azido-2,2-dimethylhexanoic acid (Kawamoto et al., 2015), 3,6,9,12,15-pentaoxaheptadecane-1,17-diamine (Jahromi et al., 2013), and (+)-biotin *N*-hydroxysuccinimide (Susumu et al., 2007) were prepared according to the reported protocols. Triethylammonium bicarbonate (TEAB) buffer at pH 7.5 was prepared freshly by bubbling CO_2 gas (from solid CO_2) into a 25 mM solution of Et_3N in purified water (Milli-Q[®], Millipore).

Purification of the synthesized molecules was performed using a Teledyne Isco combiflash instrument equipped with either a silica gel column, a C18Aq high performance RediSep[®] column, or a reversed phase high-performance liquid chromatography (HPLC) (Waters). Nuclear Magnetic Resonance (NMR) spectroscopic analyses were carried out on either a Varian INOVA 400 MHz or a Bruker Ascend 400 MHz spectrometer. ^1H NMR spectra were acquired at 400 MHz and ^{13}C NMR spectra were acquired at 100 MHz. Chemical shifts (δ) for ^1H NMR spectra were referenced to tetramethylsilane (TMS) at $\delta = 0.00$ ppm or to CD_2HCN at $\delta = 1.94$ ppm. ^{13}C NMR spectra were referenced to CDCl_3 at $\delta = 77.23$ ppm or to CD_3CN at $\delta = 118.7$ ppm. The following abbreviations are used to describe NMR resonances: s (singlet), d (doublet), t (triplet), m (multiplet), br (broad), and nfom (non-first order multiplet). Coupling constants (*J*) are reported in Hz. Low-resolution mass spectroscopy (LRMS) analysis was performed using a Bruker Daltonics Esquire 6000 mass spectrometer. Liquid chromatography followed by high-resolution mass spectroscopy (LC-HRMS) analysis in the

ESI mode was carried out on an Agilent 6520 Q-TOF or an Agilent 6230 TOF LC/MS-MS instrument.

Synthesis of (±)-(3-((*tert*-butyldimethylsilyl)oxy)-5-methoxyphenyl)(2-phenyl-1,3-dithian-2-yl)methanol, (±)-S1.



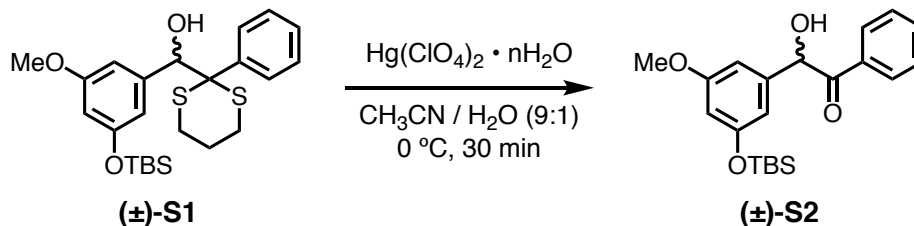
To a stirred solution of 2-phenyl-1,3-dithiane (0.8 g, 4.1 mmol, 1.1 equiv) in THF (3 mL) at -10 °C, was added 2.5 M *n*-BuLi in hexanes (1.9 mL, 4.5 mmol, 1.2 equiv) dropwise. After being stirred for 30 min, the reaction solution was treated with a solution of 3-((*tert*-butyldimethylsilyl)oxy)-5-methoxybenzaldehyde (Hurst et al., 2010) (1.0 g, 3.8 mmol, 1.0 equiv) in THF (6 mL) dropwise. The resulting mixture was stirred for 3 h at the same temperature and quenched with saturated aqueous NH₄Cl solution (10 mL). The heterogeneous mixture was extracted with EtOAc. The organic layer was washed with water and brine, dried over Na₂SO₄, and concentrated under reduced pressure. The resulting crude material was purified by combiflash silica gel chromatography (hexanes/EtOAc step gradient). The product fraction was concentrated under reduced pressure to afford the dithiane (±)-S1 (1.0 g, 61% isolated yield).

¹H NMR (400 MHz, CDCl₃) δ 7.72 (dd, *J* = 7.5, 1.5 Hz, 2H), 7.32 (dd, *J* = 7.5, 7.0 Hz, 2H), 7.40 (tt, *J* = 7.0, 1.5 Hz, 1H, overlapped), 6.25 (br t, *J* = 1.5, 1H), 6.12 (br t, *J* = 1.5, 1H), 5.89 (br t, *J* = 1.5 Hz, 1H), 4.91 (d, *J* = 4.0 Hz, 1H), 3.53 (s, 3H), 2.92 (d, *J* = 4.0 Hz, 1H), 2.78-2.62 (m, 4H), 1.97-1.90 (m, 2H), 0.94 (s, 9H), and 0.13 (s, 6H).

¹³C NMR (100 MHz, CDCl₃) δ 161.9, 158.1, 141.9, 140.1, 133.3, 130.8, 130.2, 115.5, 109.2, 108.7, 83.6, 69.0, 57.7, 30.0, 29.7, 28.3, 27.4, 20.8, and -1.7.

HRMS (ESI): calculated for [C₂₄H₃₄O₃S₂Si + (Na⁺)] 485.1611, found 485.1654.

Synthesis of (±)-2-(3-((*tert*-butyldimethylsilyl)oxy)-5-methoxyphenyl)-2-hydroxy-1-phenylethan-1-one, (±)-S2.



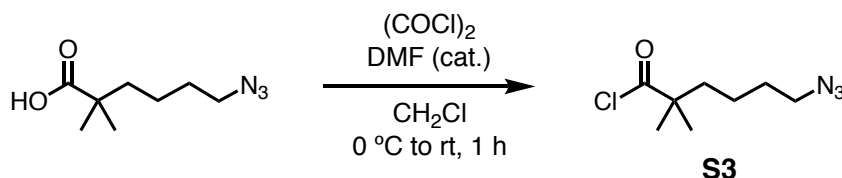
To a stirred solution of the dithiane (**(±)-S1**) (400 mg, 0.9 mmoles, 1.0 equiv) in 20 mL CH₃CN/H₂O (9:1) at 0 °C, was added Hg(ClO₄)₂·nH₂O (500 mg, 1.1 mmoles, 1.3 equiv). After being stirred for 30 min at the same temperature, the reaction mixture was quenched with 0.1 M aqueous NaHCO₃ solution. The resulting heterogenous mixture was extracted with EtOAc. The organic layer was washed with water and brine, dried over Na₂SO₄, and concentrated under reduced pressure. The resulting crude material was purified by combiflash silica gel chromatography (hexanes/EtOAc step gradient). The product fraction was concentrated under reduced pressure to afford the ketone (**(±)-S2**) (170 mg, 52% isolated yield).

¹H NMR (400 MHz, CDCl₃) δ 7.91 (dd, *J* = 7.5, 1.5 Hz, 2H), 7.53 (tt, *J* = 7.0, 1.5 Hz, 1H), 7.40 (dd, *J* = 7.5, 7.0 Hz, 2H), 6.48 (br t, *J* = 2.0 Hz, 1H), 6.39 (br t, *J* = 2.0 Hz, 1H), 6.29 (br t, *J* = 2.0 Hz, 1H), 5.82 (d, *J* = 6.0 Hz, 1H), 4.50 (d, *J* = 6.0, 1H), 3.72 (s, 3H), 0.92 (s, 9H), and 0.11 (s, 6H).

¹³C NMR (100 MHz, CDCl₃) δ 199.0, 161.3, 157.4, 141.0, 134.1, 133.7, 129.3, 129.0, 112.5, 106.6, 106.5, 76.2, 55.5, 25.8, 18.4, and -4.3.

HRMS (ESI): calculated for [C₂₁H₂₈O₄Si + (Na⁺)] 395.1649, found 395.1672.

Synthesis of 6-azido-2,2-dimethylhexanoyl chloride, S3.



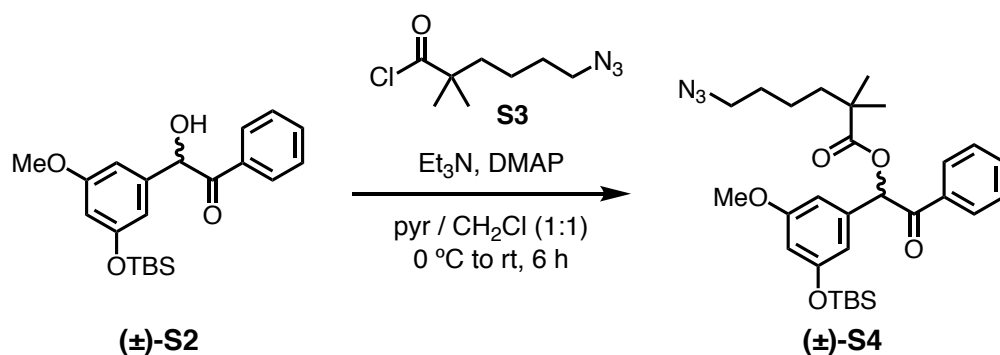
To a stirred solution of 6-azido-2,2-dimethylhexanoic acid (Kawamoto et al., 2015) (300 mg, 1.6 mmoles, 1.0 equiv) in CH₂Cl₂ (3 mL) at 0 °C, was sequentially added (COCl)₂ (160 μL, 1.9 mmoles, 1.2 equiv) and DMF (20 μL, catalytic amount). The reaction mixture was

stirred at the same temperature for 1 h. The resulting mixture was then filtered through a PTFE filter (0.2 μm) and the filtrate was concentrated under reduced pressure to remove all volatiles. The residue essentially contained the hexanoyl chloride **S3**, which was used immediately in the next step without purification.

$^1\text{H NMR}$ (400 MHz, CDCl_3) δ 3.30 (t, $J = 7.0$ Hz, 2H), 1.70-1.64 (mfom, 2H), 1.61 (tt, $J = 7.5$, 7.0 Hz, 2H), 1.42-1.34 (m, 2H), and 1.31 (s, 6H).

$^{13}\text{C NMR}$ (100 MHz, CDCl_3) δ 180.0, 52.8, 51.1, 39.8, 29.1, 25.2, and 22.0.

Synthesis of (\pm)-1-(3-((*tert*-butyldimethylsilyl)oxy)-5-methoxyphenyl)-2-oxo-2-phenylethyl 6-azido-2,2-dimethylhexanoate, (\pm)-**S4**.



To a stirred solution of the benzoin (\pm)-**S2** (140 mg, 0.38 mmoles, 1.0 equiv) in 2 mL of pyridine / CH_2Cl_2 (1:1) at 0 °C, was added Et_3N (30 μL , 0.20 mmoles, 0.5 equiv) and DMAP (19 mg, 0.15 mmoles, 0.4 equiv). After being stirred for 10 min, the reaction solution was treated with a solution of the hexanoyl chloride **S3** (93 mg, 0.46 mmoles, 1.2 equiv) in CH_2Cl_2 (200 μL). The resulting mixture was stirred for 6 h at the same temperature and quenched with saturated aqueous NaHCO_3 solution (2 mL). The heterogenous mixture was extracted with EtOAc . The organic layer was washed with water and brine, dried over Na_2SO_4 , and concentrated under reduced pressure. The resulting crude material was purified by combiflash silica gel chromatography (hexanes/ EtOAc step gradient). The product fraction was concentrated under reduced pressure to afford the benzoin ester (\pm)-**S4** (185 mg, 91% isolated yield).

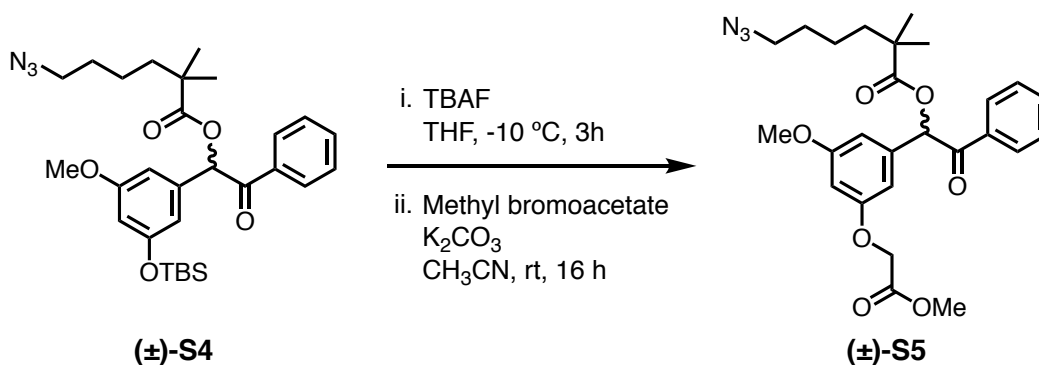
$^1\text{H NMR}$ (400 MHz, CDCl_3) δ 7.71 (dd, $J = 7.5$, 1.5 Hz, 2H), 7.29 (tt, $J = 7.0$, 1.5 Hz, 1H), 7.18 (dd, $J = 7.5$, 7.0 Hz, 2H), 6.47 (s, 1H), 6.39 (br t, $J = 2.0$ Hz, 1H), 6.30 (br t, $J = 2.0$ Hz, 1H),

6.13 (br t, $J = 2.0$ Hz, 1H), 3.53 (s, 3H), 3.03 (t, $J = 7.0$, 2H), 1.47-1.31 (m, 2H + 2H, overlapped), 1.25-1.09 (m, 2H), 1.05 (s, 3H), 1.04 (s, 3H), 0.73 (s, 9H), and -0.10 (s, 6H).

$^{13}\text{C NMR}$ (100 MHz, CDCl_3) δ 194.2, 177.4, 161.2, 157.3, 135.8, 135.1, 133.5, 129.0, 128.8, 112.7, 107.3, 106.9, 76.9, 55.5, 51.5, 42.5, 40.2, 29.5, 25.9, 25.3, 25.2, 22.3, 18.4, and -4.3.

HRMS (ESI): calculated for $[\text{C}_{29}\text{H}_{41}\text{N}_3\text{O}_5\text{Si} + (\text{H}^+)]$ 540.2888, found 540.2907.

Synthesis of (\pm)-1-(3-methoxy-5-(2-methoxy-2-oxoethoxy)phenyl)-2-oxo-2-phenylethyl 6-azido-2,2-dimethylhexanoate, (\pm)-**S5**.



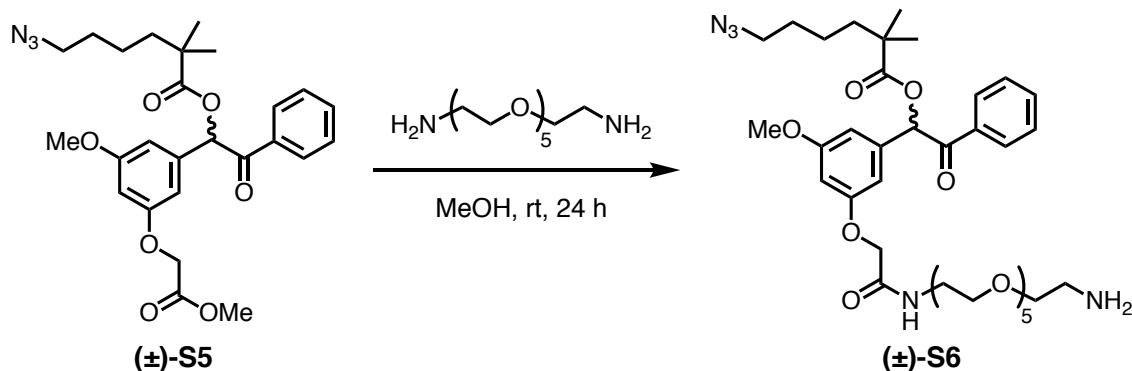
To a stirred solution of the benzoin ester (\pm)-**S4** (90 mg, 0.17 mmoles, 1.0 equiv) in THF (3 mL) at -10 °C, was added a 1.0 M THF solution of TBAF (180 μL , 0.18 mmoles, 1.1 equiv) dropwise. After being stirred for 3 h at the same temperature, the reaction solution was treated with a solution of methyl bromoacetate (20 μL , 0.2 mmoles, 1.2 equiv) in CH_3CN (1 mL) followed by K_2CO_3 (23 mg, 0.17 mmoles, 1.0 equiv). The resulting mixture was stirred at room temperature for 16 h and quenched at 0 °C with saturated aqueous NH_4Cl solution (5 mL). The heterogenous mixture was extracted with EtOAc. The organic layer was washed with water and brine, dried over Na_2SO_4 , and concentrated under reduced pressure. The resulting crude material was purified by combiflash silica gel chromatography (hexanes / EtOAc step gradient). The product fraction was concentrated under reduced pressure to afford the methyl ester (\pm)-**S5** (50 mg, 59% isolated yield).

$^1\text{H NMR}$ (400 MHz, CDCl_3) δ 7.91 (dd, $J = 8.0$, 1.5 Hz, 2H), 7.53 (tt, $J = 7.5$, 1.5 Hz, 1H), 7.41 (dd, $J = 8.0$, 7.5 Hz, 2H), 6.69 (s, 1H), 6.64 (br t, $J = 2.0$ Hz, 1H), 6.58 (br t, $J = 2.0$ Hz, 1H), 6.43 (br t, $J = 2.0$ Hz, 1H), 4.58 (s, 2H), 3.78 (s, 3H), 3.75 (s, 3H), 3.24 (t, $J = 7.0$, 2H), 1.67-1.51 (m, 2H + 2H, overlapped), 1.43-1.27 (m, 2H), 1.25 (s, 3H), and 1.24 (s, 3H).

¹³C NMR (100 MHz, CDCl₃) δ 194.1, 177.4, 169.1, 161.3, 159.4, 136.2, 135.0, 133.7, 129.0, 128.9, 107.8, 106.8, 101.8, 77.3, 65.5, 55.7, 52.5, 51.5, 42.5, 40.2, 29.5, 25.3, 25.2, and 22.3.

HRMS (ESI): calculated for [C₂₆H₃₁N₃O₇ + (H⁺)] 498.2235, found 498.2250.

Synthesis of (±)-1-(3-methoxy-5-(2-methoxy-2-oxoethoxy)phenyl)-2-oxo-2-phenylethyl 6-azido-2,2-dimethylhexanoate, (±)-S6.



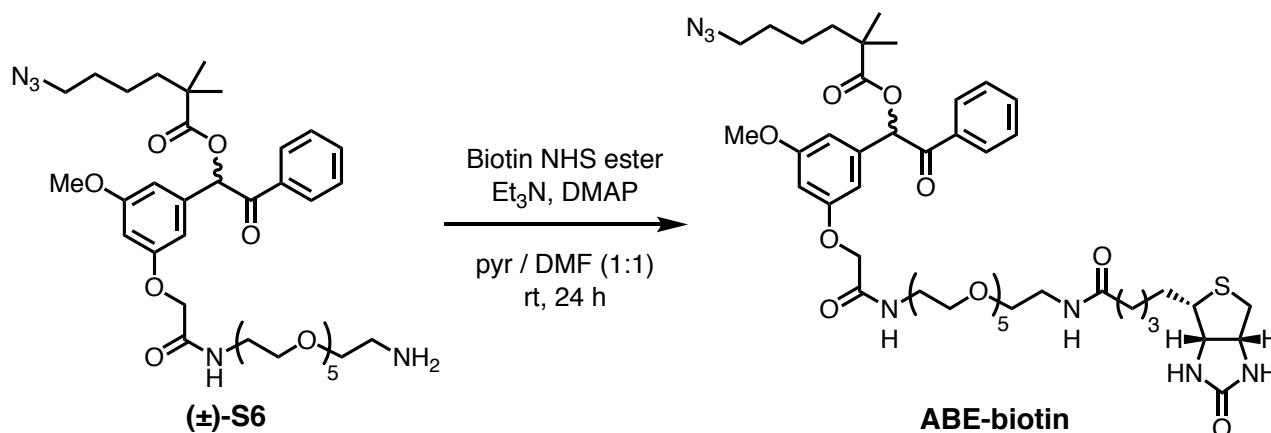
To a stirred solution of the methyl ester **(±)-S5** (50 mg, 0.1 mmoles, 1 equiv) in MeOH (500 μL) at room temperature, was added 3,6,9,12,15-pentaoxaheptadecane-1,17-diamine (Jahromi et al., 2013) (110 mg, 0.4 mmoles, 4 equiv). The reaction mixture was stirred for 24 h and concentrated to viscous oil under reduced pressure. The crude material was purified by combiflash silica gel chromatography (CH₂Cl₂/MeOH step gradient). The product fraction was concentrated under reduced pressure to afford the amine **(±)-S6** (60 mg, 81% isolated yield).

¹H NMR (400 MHz, CD₃CN) δ 8.41 (br s, 1H), 7.97 (dd, *J* = 7.5, 1.5 Hz, 2H), 7.59 (tt, *J* = 7.5, 1.5 Hz, 1H), 7.49 (dd, *J* = 7.5, 7.5 Hz, 2H), 6.77 (s, 1H), 6.69 (br t, *J* = 2.0 Hz, 1H), 6.67 (br t, *J* = 2.0 Hz, 1H), 6.53 (br t, *J* = 2.0 Hz, 1H), 4.44 (s, 2H), 3.97 (br s, 2H), 3.75 (s, 3H), 3.65 (dd, *J* = 5.0, 5.0 Hz, 2H), 3.62-3.49 (m, 18H), 3.40 (d, *J* = 5.5, 1H), 3.38 (d, *J* = 5.5, 1H), 3.26 (t, *J* = 7.0, 2H), 3.00 (dd, *J* = 5.0, 5.0 Hz, 2H), 1.63-1.48 (m, 2H + 2H, overlapped), 1.44-1.25 (m, 2H), 1.22 (s, 3H), and 1.20 (s, 3H).

¹³C NMR (100 MHz, CD₃CN) δ 196.7, 179.5, 170.8, 168.4, 163.9, 161.8, 139.0, 137.2, 136.5, 131.6, 131.2, 110.0, 109.7, 103.9, 79.6, 72.6, 72.52/72.51, 72.44/72.38, 72.3, 72.2, 72.1, 72.0, 70.2, 69.8, 57.9, 53.6, 44.6, 42.4, 42.3, 41.0, 31.6, 27.1, and 27.0.

HRMS (ESI): calculated for [C₃₇H₅₅N₅O₁₁ + (H⁺)] 746.3971, found 746.4004.

Synthesis of the photocleavable probe, azido benzoin ester (ABE)-biotin.



To a stirred solution of the amine (**±**)-S6 (50 mg, 0.07 mmoles, 1.0 equiv) in 1 mL of pyridine/CH₂Cl₂ (1:1) at room temperature, was added Et₃N (15 μL, 0.10 mmoles, 1.5 equiv), DMAP (4 mg, 0.03 mmoles, 0.5 equiv), and (+)-biotin *N*-hydroxysuccinimide (NHS) ester (27 mg, 0.08 mmoles, 1.2 equiv), which was prepared from *d*-biotin and *N*-hydroxysuccinimide (Susumu et al., 2007). The resulting mixture was stirred for 24 h at the same temperature and quenched with half-saturated brine (1 mL). The heterogenous mixture was extracted with EtOAc. The organic layer was dried over Na₂SO₄, and concentrated under reduced pressure. The crude material was purified first by combiflash silica gel chromatography (CH₂Cl₂ / MeOH step gradient) and then by reversed phase HPLC [gradient elution between (A) aqueous 25 mM TEAB buffer (pH 7.5) and (B) CH₃CN] to afford a diastereomeric mixture of the desired photocleavable probe **ABE-biotin** (35 mg, 54% isolated yield).

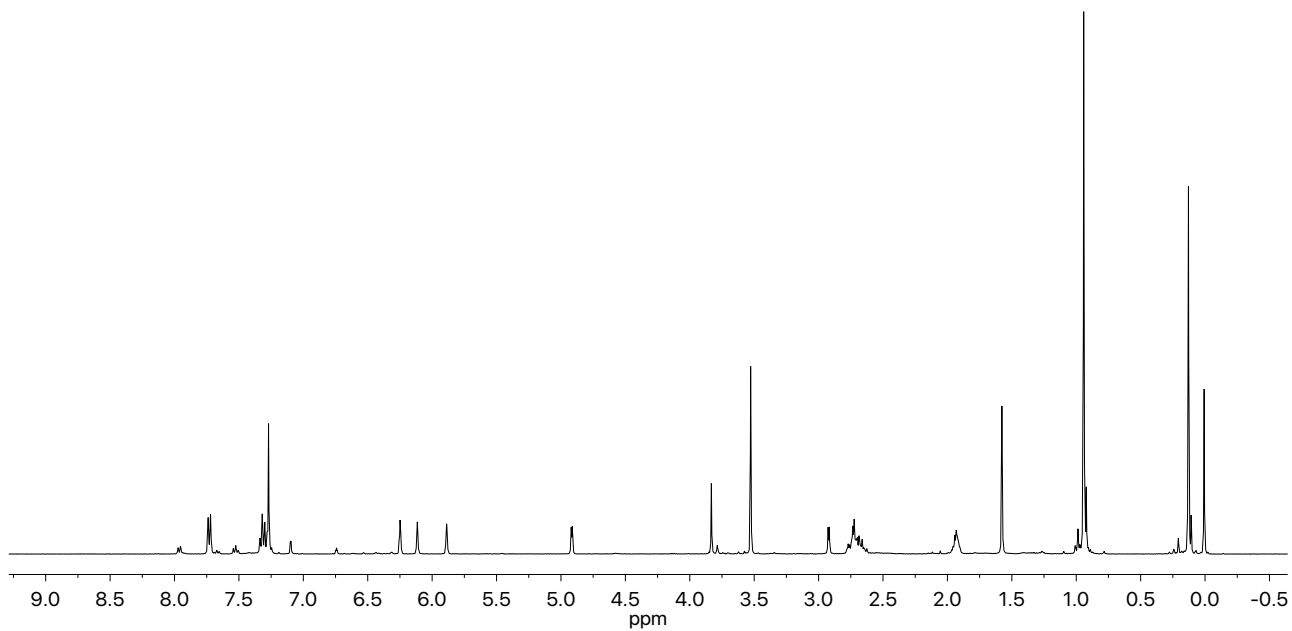
¹H NMR (400 MHz, CD₃CN) δ 8.14 (s, 1H), 7.97 (dd, *J* = 7.5, 1.5 Hz, 2H), 7.62 (tt, *J* = 7.5, 1.5 Hz, 1H), 7.50 (dd, *J* = 7.5, 7.5 Hz, 2H), 7.16 (br t, *J* = 5.0, 1H), 6.78 (s, 1H), 6.70 (br t, *J* = 2.0 Hz, 1H), 6.68 (br t, *J* = 2.0 Hz, 1H), 6.59 (br t, *J* = 2.0 Hz, 1H), 6.52 (t, *J* = 2.0, 1H), 5.43 (br s, 1H), 5.15 (br s, 1H), 4.44 (s, 2H), 4.41 (m, 1H), 4.24 (ddd, *J* = 6.0, 4.5, 1.5 Hz, 1H), 3.76 (s, 3H), 3.56-3.52 (m, 16H), 3.48 (t, *J* = 6.0, 2H), 3.46 (t, *J* = 6.0, 2H), 3.39 (t, *J* = 6.0, 1H), 3.38 (t, *J* = 6.0, 1H), 3.30 (t, *J* = 6.0, 2H), 3.27 (t, *J* = 7.0, 2H), 3.15 (ddd, *J* = 8.0, 7.0, 4.5, 1H), 2.88 (dd, *J* = 12.5, 5.0, 1H), 2.64 (d, *J* = 12.5, 1H), 2.14 (t, *J* = 7.5, 2H), 1.73-1.48 (m, 7H), 1.44-1.26 (m, 4H), 1.23 (s, 3H), and 1.21 (s, 3H).

¹³C NMR (100 MHz, CD₃CN) δ 195.1, 177.9, 174.0, 168.8, 164.1, 163.9, 162.3, 160.2, 137.4, 135.7, 134.9, 130.0, 129.7, 108.5, 108.1, 102.3, 78.0, 71.2, 71.19/71.18, 71.1, 71.00/70.96,

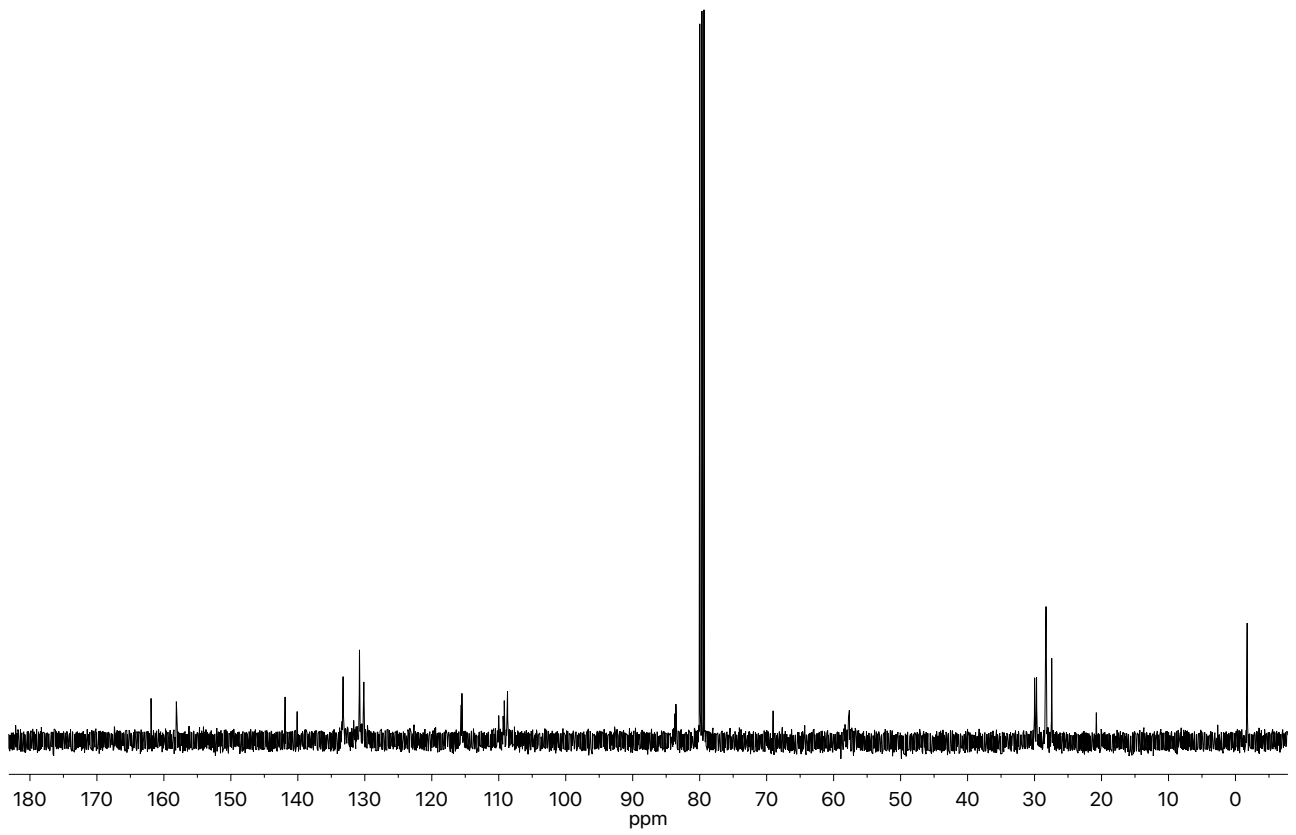
70.5, 70.2, 68.3, 62.5, 60.9, 56.4, 56.3, 52.0, 43.0, 41.2, 40.8, 39.9, 39.5, 36.4, 30.0, 29.08/29.05, 26.5, 25.49/25.47, and 22.9.

HRMS (ESI): calculated for $[C_{47}H_{69}N_7O_{13}S + (H^+)]$ 972.4747, found 972.4775.

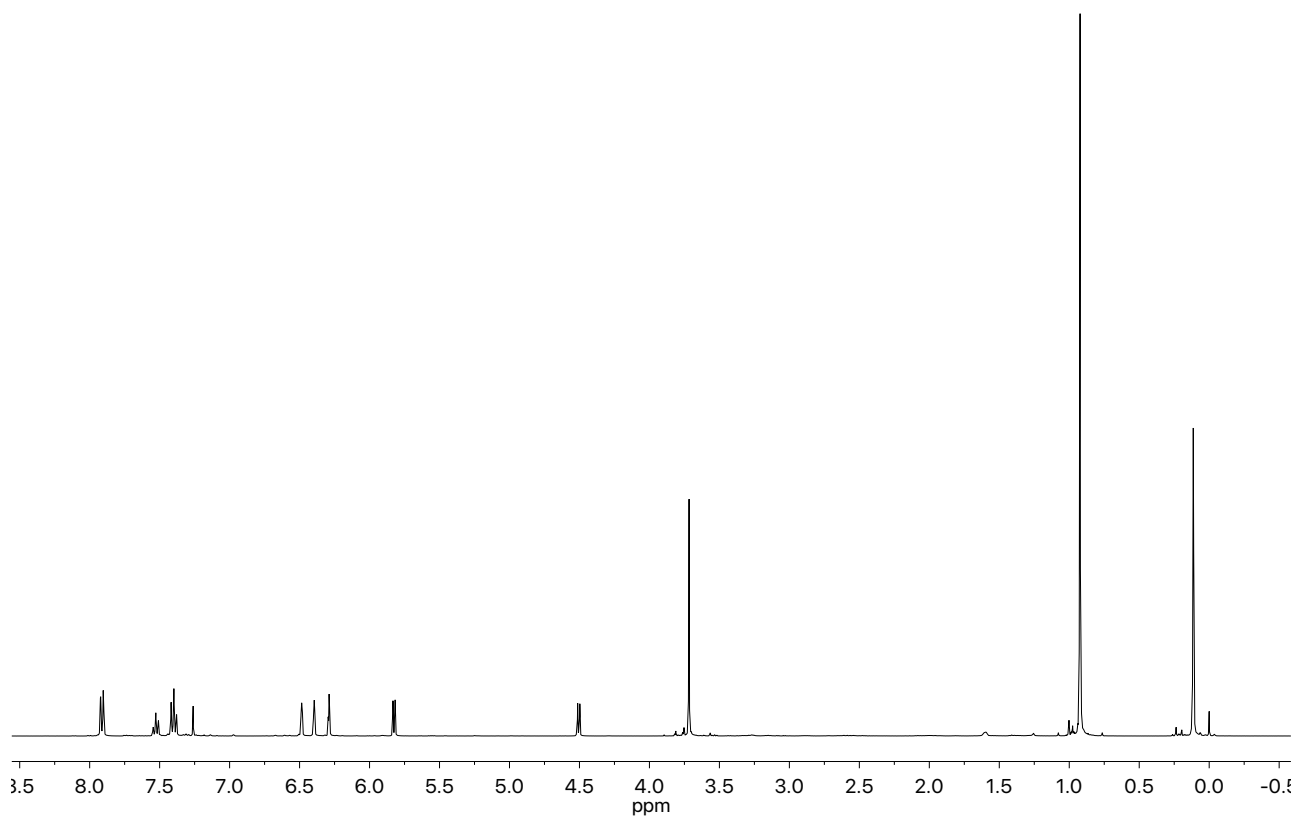
(±)-S1 (1H NMR: 400 MHz, $CDCl_3$)



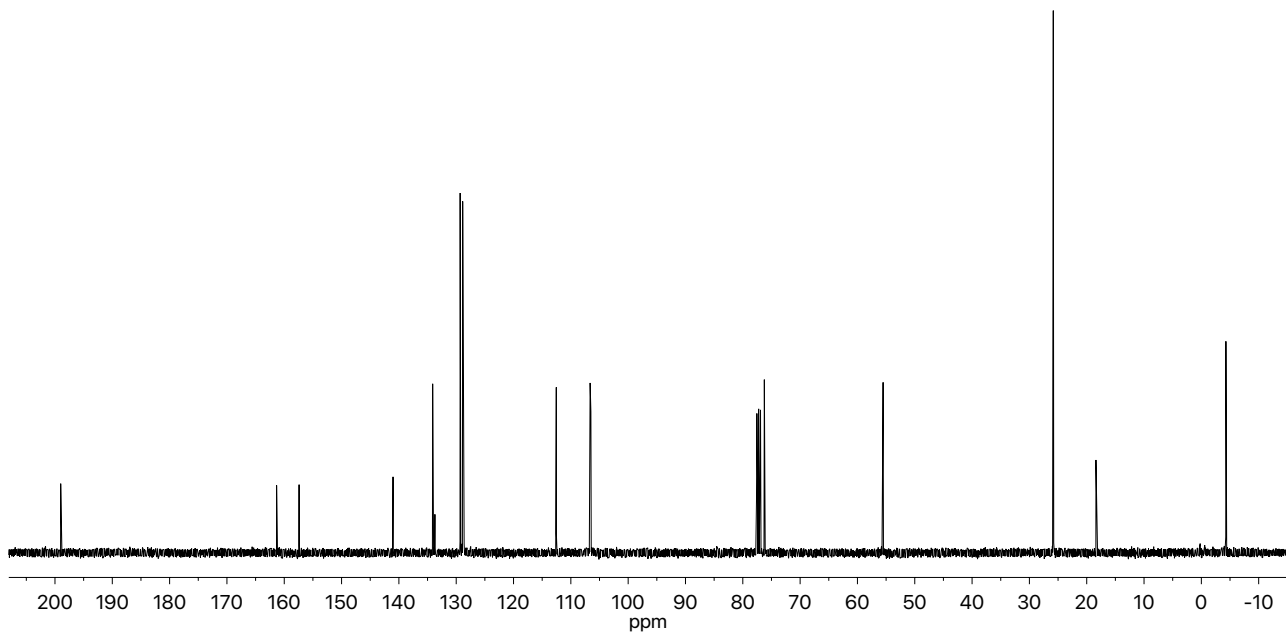
(±)-S1 (^{13}C NMR: 100 MHz, $CDCl_3$)



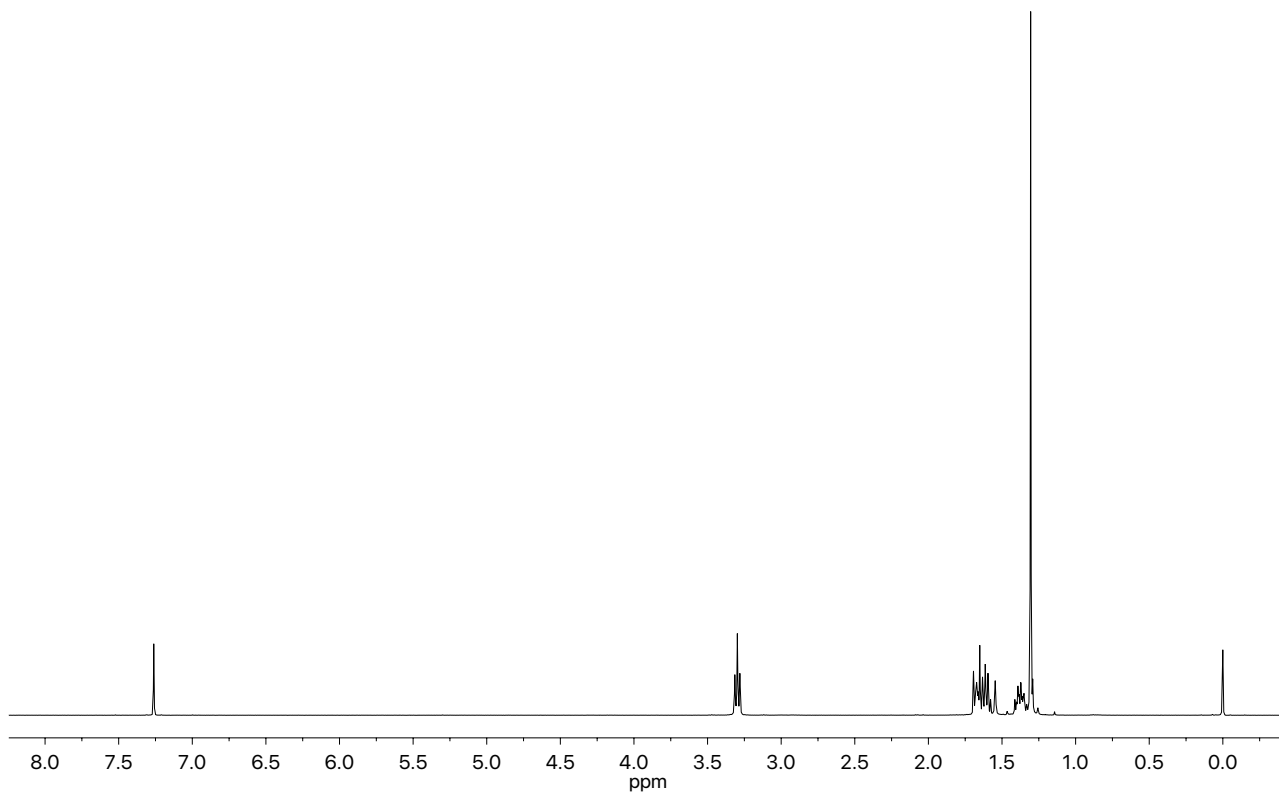
(±)-S2 (¹H NMR: 400 MHz, CDCl₃)



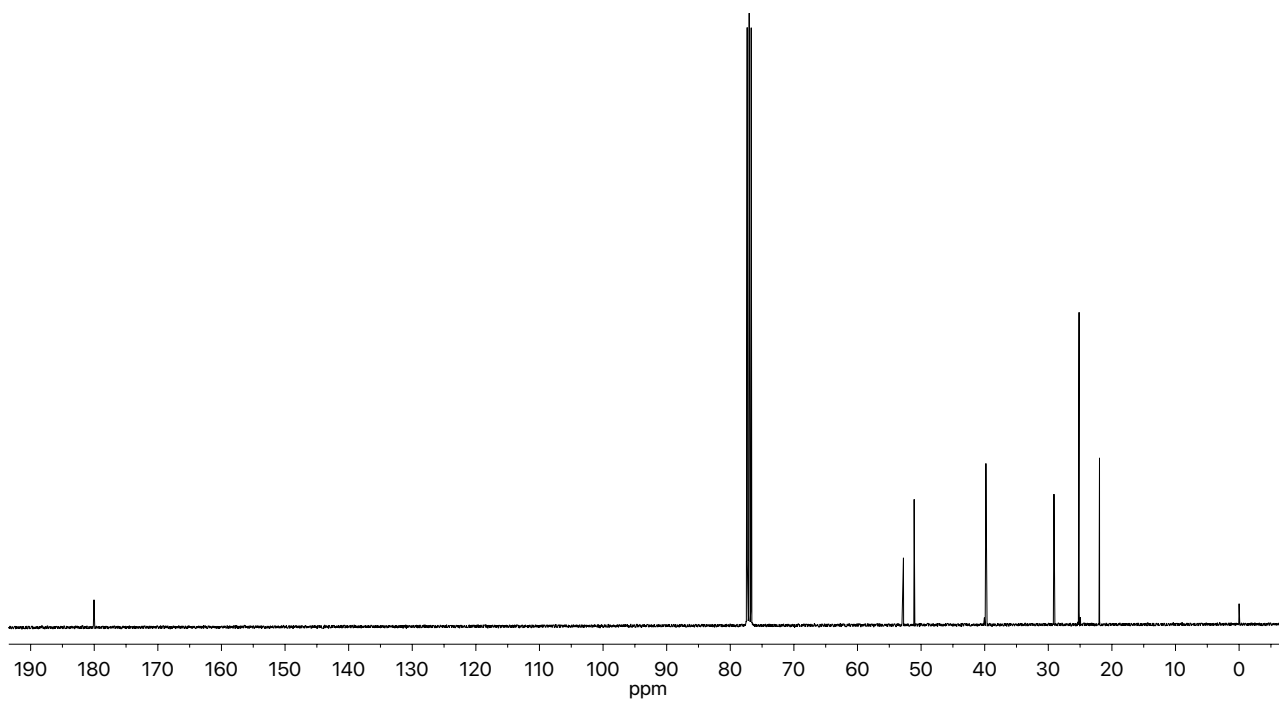
(±)-S2 (¹³C NMR: 100 MHz, CDCl₃)



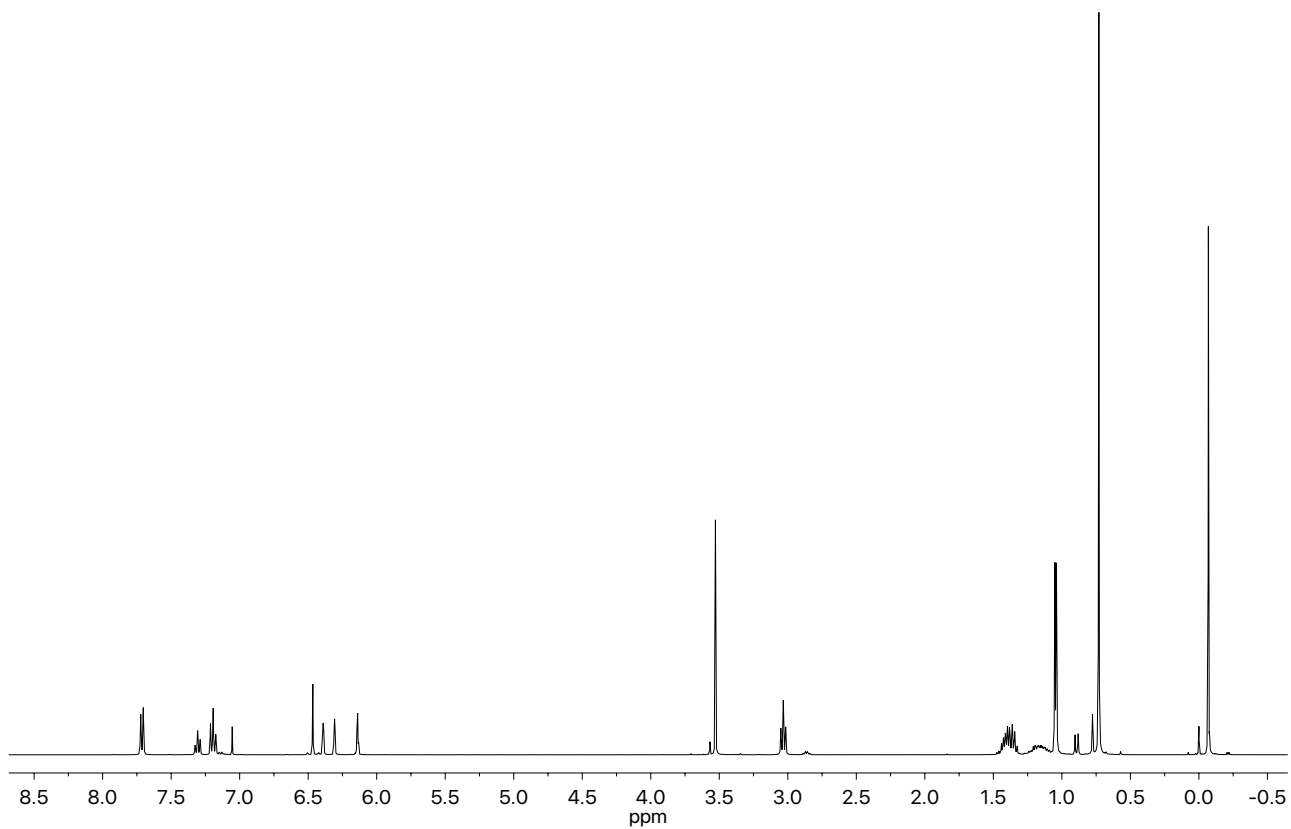
(±)-S3 (^1H NMR: 400 MHz, CDCl_3)



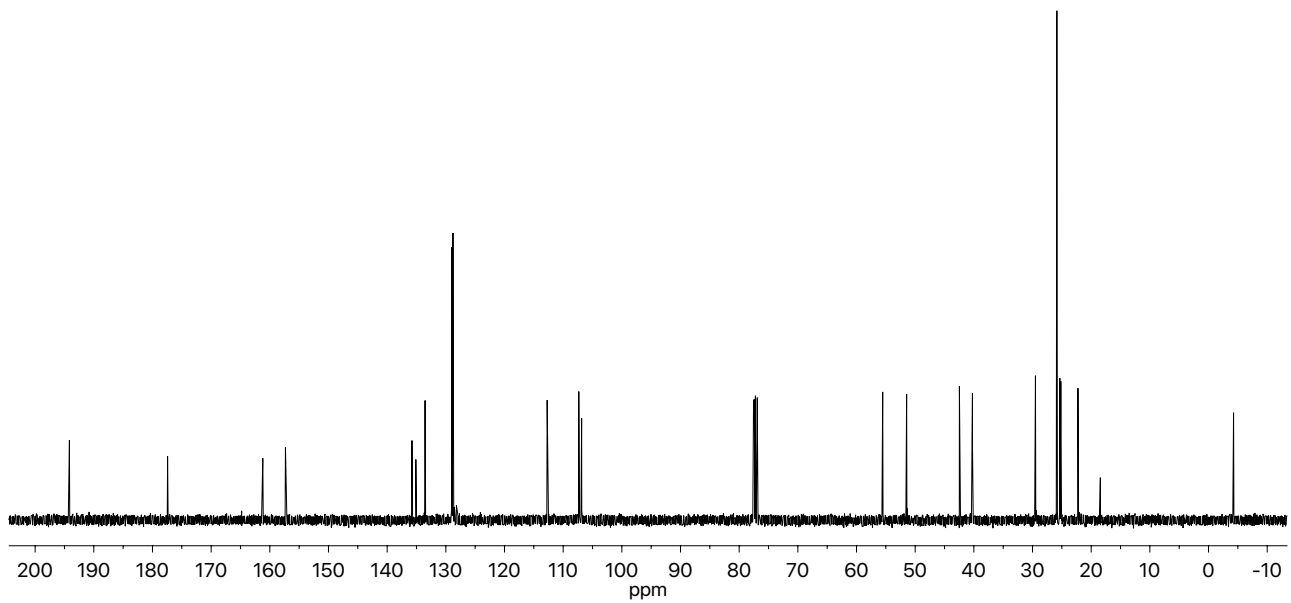
(±)-S3 (^{13}C NMR: 100 MHz, CDCl_3)



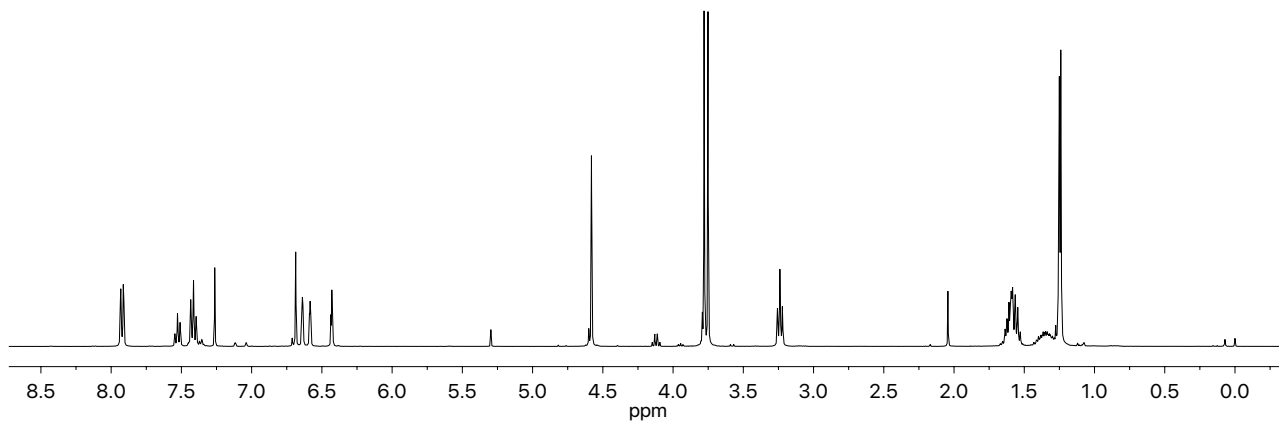
(±)-S4 (^1H NMR: 400 MHz, CDCl_3)



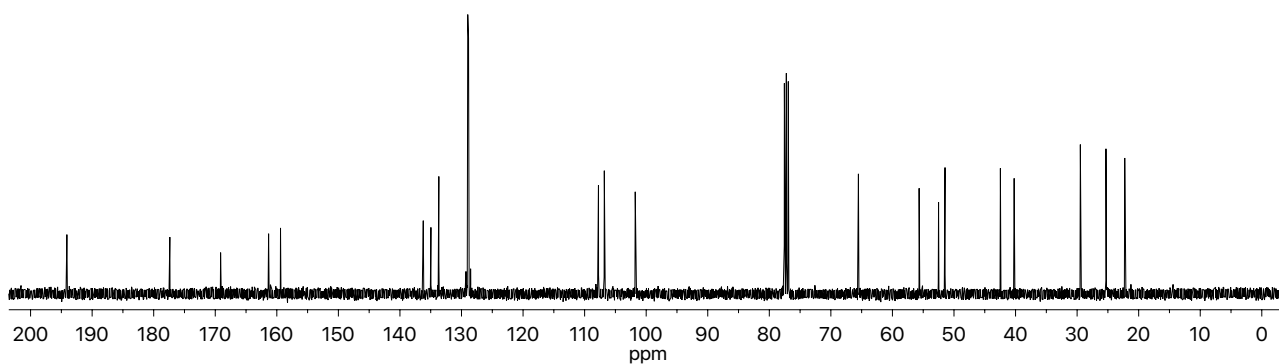
(±)-S4 (^{13}C NMR: 100 MHz, CDCl_3)



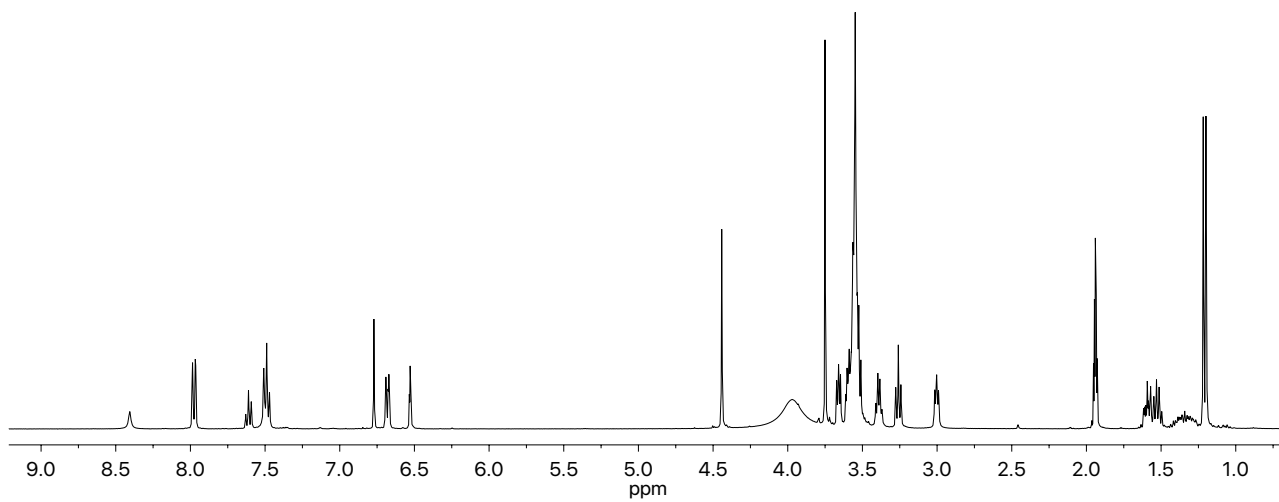
(±)-S5 (^1H NMR: 400 MHz, CDCl_3)



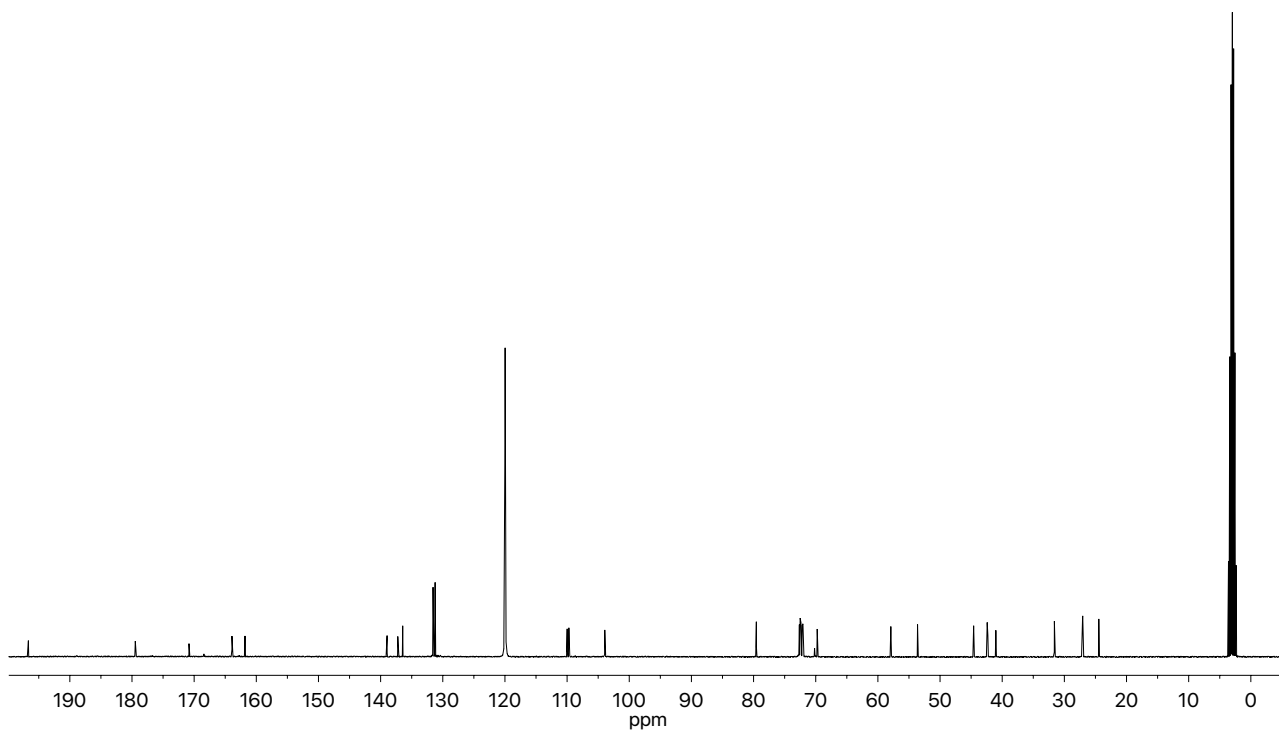
(±)-S5 (^{13}C NMR: 100 MHz, CDCl_3)



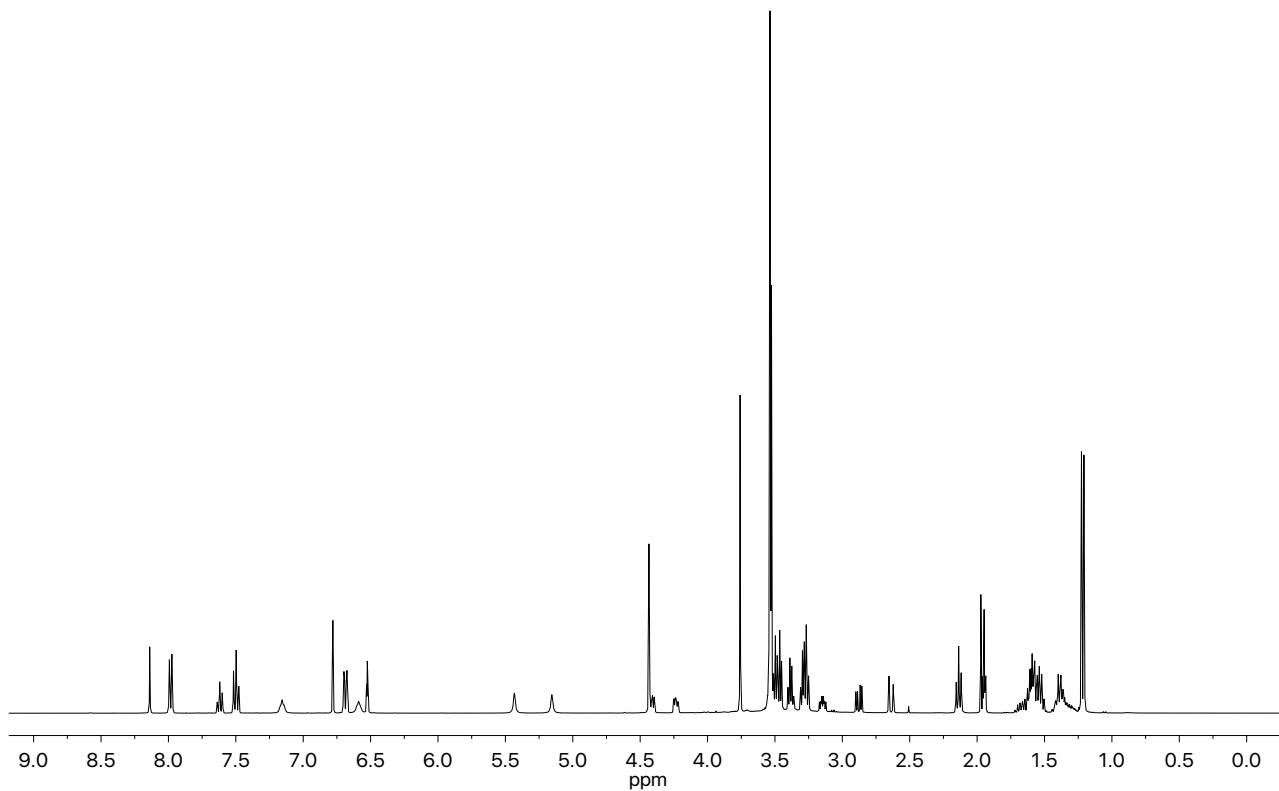
(±)-S6 (^1H NMR: 400 MHz, CD_3CN)



(±)-S6 (^{13}C NMR: 100 MHz, CD_3CN)



ABE-biotin (^1H NMR: 400 MHz, CD_3CN)



ABE-biotin (^{13}C NMR: 100 MHz, CD_3CN)

